Electronic Supplementary Material (ESI) for Dalton Transactions.
This journal is © The Royal Society of Chemistry 2022

Supplementary Information for Synthesis and Reactivity of Titanium POCOP Pincer Complexes

*Leah Webster[1], Tobias Krämer[2] and Mark Chadwick[1]**

[1] Molecular Sciences Research Hub, Imperial College London, 82 Wood Lane, London, W12 0BZ, UK.

[2] Department of Chemistry, Maynooth University, Maynooth, Co. Kildare, Ireland.

Email: m.chadwick@imperial.ac.uk

Experimental

1. Experimental

1.1 General Considerations

Unless otherwise stated all manipulations were carried out under an inert atmosphere (N_2) using standard dual-manifold Schlenk techniques or employment of an MBraun Labmaster glovebox. Glassware was dried in an over at 180°C overnight before use. Anhydrous solvents (toluene, pentane, hexane) were obtained from a Grubbs type SPS system and stored over potassium mirrors under inert atmosphere. THF and Et_2O were dried by refluxing over Solvona^{TM} and stored over activated 3 Å molecular sieves or potassium mirror respectively, whilst being kept under inert atmosphere. All other solvents, including deuterated solvents, were dried by being stored over activated 3 Å molecular sieves and subsequent degassing by three freeze-pump-thaw cycles.

Solution NMR data were collected on either a Brucker 400 MHz or 500 MHz spectrometer employing NMR tubes fitted with a J. Young's style stopcock. Data were collected at room temperature unless stated otherwise. Variable temperature data were collected by Mr Pete Haycock or Dr Stuart Elliot. Chemical shifts (δ) are stated in PPM and referenced internally to residual solvent protio-resonances (^{1}H) or externally to 85% H_3PO_4 (^{31}P) or LiCl (^{7}Li). Coupling constants (J) are quoted in Hz. Evan's method calculations were performed with a known concentration of sample in C_6D_6 and an external reference capillary of C_6D_6 doped with C_6H_6 (20 µL C_6H_6 in 1 mL of C_6D_6). The spectra were collected using a standard ^{1}H experiment. Calculation of the effective magnetic moment was then calculated with the equation initially reported by E. Schubert.[1] The data was processed using Mestrenova.

Single crystal x-ray diffraction data were collected as follows: a typical crystal was mounted on a MiTeGen Micromounts using perfluoropolyether oil and cooled rapidly to 173 K in a stream of nitrogen gas using a cryostream unit. Data were collected with an Agilent Diffraction Xcalibur PX Ultra A and Xcalibur 3E diffractometers (Cu Kα radiation, λ = 1.54180 Å). Raw frame data were reduced using CrysAlisPro.[2] The structures were solved using SuperFlip and refined using full-matrix least squares refinement on all F^2 data using the CRYSTALS program suite.[3–5] In general distances and angles were calculated using the full covariance matrix

Room temperature X Band CW EPR measurements were collected on a Magnettech ESR5000 Benchtop CW X band spectrometer. X Band EPR measurements were conducted with 10 mW microwave power, 100 kHz modulation frequency and 0.2 mT modulation amplitude. The Q-band EPR measurements were performed at room temperature on an Elexsys E580 spectrometer (Bruker) equipped with an ER 5106QT-2w microwave resonator (Bruker). The spectrum was recorded using a microwave power of 0.1 mW, a field modulation amplitude of 0.75 G, a field modulation frequency of 100 kHz, a conversion time of 29.30 ms and a sweep rate of 4.2 G/s; 4 scans were accumulated. All data analysis was carried out using EasySpin.[6]

Infrared spectra were obtained on a Cary630 spectrometer (placed within a MBraun glovebox) from crystalline solids.

$TiCl_4(THF)_2$, $TiCl_3(THF)_3$, ^{tBu}POCOP-Br, ^{iPr}POCOP-Br and neopentyl lithium were prepared by literature procedures.[7–9] ^{n}BuLi, MeMgCl and PhMgCl were purchased

from Sigma Aldrich and titrated against cyclooctadiene following the procedure by T. Hoye.[10] *Tert*-butyl lithium solution was purchased from Sigma Aldrich, dried under vacuum and used as a solid. All other chemicals were obtained from commercial suppliers (Sigma-Aldrich, Fluorochem, TCI) and used as purchased. Dihydrogen was purchased from CK isotopes and used as received.

1.2 ^{tBu}POCOP-Li

^{tBu}POCOP-Br (1 g, 2.09 mmol, 1 equiv.) was dissolved in pentane and cooled to −78°C. ^{n}BuLi (2.5M, 0.92 mL, 1.1 equiv.) was added and the reaction mixture was warmed to room temperature and stirred for 2 hours. Solvents were removed *in vacuo* to yield a colourless solid. (0.841 g, 99%)

^{1}H NMR (400 MHz, C_6D_6): δ 7.21 (m, 3H), 1.15 (d, 36H).

^{31}P{^{1}H} NMR (162 MHz, C_6D_6): δ 142.9 (s, br).

^{7}Li NMR (156 MHz, C_6D_6): δ 3.5 (quintet).

1.3 ^{iPr}POCOP-Li

^{iPr}POCOP-Br (200 mg, 0.48 mmol, 1 equiv.) was dissolved in pentane and cooled to −78°C. ^{t}BuLi (64 mg, 1 mmol, 2.1 equiv.) was dissolved in pentane and added to the solution of ^{iPr}POCOP-Br. The reaction mixture was warmed to room temperature and stirred for 2 hours. The solution was filtered away from any LiBr formed and the solution used subsequently without any further purification assuming 100% yield.

^{1}H NMR (400 MHz, C_6D_6): δ 7.21 (m, 3H), 1.85 (sept 4H), 1.11 (dd 12H), 0.98 (dd, 12H)

^{31}P{^{1}H} NMR (162 MHz, C_6D_6): δ 131.5 (s).

^{7}Li NMR (156 MHz, pentane with C_6D_6 insert): δ 3.83 (quint)

1.4 (^{tBu}POCOP)$TiCl_2$ (1)

An analogous preparation was previously reported, however with minimal characterisation.[11] $TiCl_3(THF)_3$ (449 mg, 1.21 mmol, 1 equiv.) was suspended in pentane and cooled to −78°C. A pentane solution of ^{tBu}POCOP-Li (490 mg, 1.21 mmol, 1 equiv.) was added and the mixture allowed to warm to room temperature and stirred overnight. The resultant blue solution was filtered, and solvents removed *in vacuo.* The product was extracted into pentane, filtered and solvents removed *in vacuo*; yielding (^{tBu}POCOP)$TiCl_2$ as a blue solid (372 mg, 59%). Crystals suitable for x-ray crystallography were grown from a saturated cyclopentane solution cooled to −40°C, however the structure (grown from toluene) has been previously reported (CCDC 2169339).

NMR analysis is limited to ^{1}H NMR spectroscopy due to the paramagnetic nature of the compound.

Elemental Analysis found (calculated for $C_{22}H_{39}Cl_2O_2P_2Ti$): C 51.31 (51.18), H 7.49 (7.61)

^{1}H NMR (400 MHz, C_6D_6): δ 10.39 (s, br), 2.68 (s,br).

^{31}P{^{1}H} NMR (162 MHz, C_6D_6): No resonances observed.

IR (solid state): 2956, 2895, 2864, 1578, 1545, 1472, 1460, 1414, 1397, 1368, 1261, 1220, 1202, 1195, 1181, 1077, 1019, 1007, 970, 932, 867, 806, 777, 719, 704, 619, 565, 485, 427, 405.

μ_{eff} (Evan's method): 1.86 μ_B

X Band CW EPR (303 K, toluene): Major: 95% g_{iso}= 1.9665, hyperfine coupling to two ^{31}P nuclei (a_0= 2.31 mT). Minor: 5% g_{iso}= 1.9720, hyperfine coupling to two ^{31}P nuclei (a_0= 2.22 mT)

1.5 (^{tBu}POCOP)$TiCl_3$ (2)

^{tBu}POCOP-Li (0.6419 g, 1.59 mmol, 1 equiv.) was dissolved in pentane and cooled to −78 °C. $TiCl_4$ (175 µL, 1.59 mmol, 1 equiv.) in pentane was added dropwise to the solution which immediately changed from colourless to brick red. The mixture was warmed to room temperature and stirred for 2 hours. Solvents were removed in vacuo and the product extracted in Et_2O and filtered. Solvents were removed in vacuo and the red solid was washed with pentane at 0°C, yielding (^{tBu}POCOP)$TiCl_3$ as a red solid (57%, 0.498 g). Crystals suitable for x-ray diffraction were grown from a hexane solution at −40°C.

^{1}H NMR (400 MHz, C_6D_6): δ 6.85 (t, 1H, J =7.90 Hz, $CH_{aryl\text{-}para}$), 6.56 (d, 2H, J = 8 Hz, $CH_{aryl\text{-}meta}$), 1.41 (d, 36H, J = 13 Hz, $C(C\underline{H}_3)_3$).

^{31}P{^{1}H} NMR (162 MHz, C_6D_6): δ 187.6.

^{13}C{^{1}H} NMR (101 MHz, C_6D_6): 165.2 (s, $C_{aryl\text{-}ortho}$), 134.2 (s, $C_{aryl\text{-}para}$), 108.5 (s, $C_{aryl\text{-}meta}$), 41.4 (s, $\underline{C}(CH_3)_3$), 29.0 (s, $C(\underline{C}H_3)_3$). Resonances for $C_{aryl\text{-}ipso}$ not observed.

IR (solid state): 2961, 2871, 1569, 1470, 1441, 1400, 1372, 1258, 1232, 1176, 1057, 1027, 990, 937, 911, 865, 811, 688, 647, 518

1.6 (^{tBu}POCOP*)$_2TiCl_2$ (3)

$TiCl_4(THF)_2$ (206 mg, 0.608 mmol, 1 equiv.) in THF was cooled to −78 °C and a cooled pentane solution of ^{tBu}POCOP-Li (500 mg, 1.236 mmol, 2 equiv) was added. The mixture was warmed to room temp and stirred overnight; changing from a yellow solution to a dark red mixture. Solvents were removed in vacuo and the product extracted in toluene and filtered through celite. Solvents were removed in vacuo and the product washed with pentane at 0 °C and dried *in vacuo.* This yielded (^{tBu}POCOP*)$_2TiCl_2$ as an orange powder (171 mg, 31%) Orange crystals suitable for x-ray crystallography were grown from a saturated hexane solution cooled to −40°C.

^{1}H NMR (400 MHz, C_6D_6): δ 8.20 (dd, 1H, J = 8 Hz, 12 Hz, CH_{aryl}), 7.05 (t, 1H, J = 8 Hz, $CH_{aryl\text{-}para}$), 6.45 (d, 1H, J= 8.4 Hz, CH_{aryl}), 1.76 (br, 18H, $P(C(CH_3)_3)_2$), 1.10 (d, 18H, J = 12 Hz, $O\text{-}P(C(CH_3)_3)_2$).

^{13}C{^{1}H} NMR (101 MHz, C_6D_6): δ 175.6 (t, J = 13 Hz, C_{aryl}), 164.6 (d, J = 10 Hz, C_{aryl}), 132.6 (d, J = 3Hz, C_{aryl}), 112.7 (s C_{aryl}), 111.92 (t, J = 9 Hz, C C_{aryl}), 108.0 (s, C_{aryl}),

36.20 (s, Ti-P<u>C</u>$(CH_3)_3$), 35.86 (s, Ti-P<u>C</u>$(CH_3)_3$), 31.70 (s, OP<u>C</u>$(CH_3)_3$), 29.99 (d, J = 4 Hz, Ti-PC($\underline{C}H_3)_3$), 28.69 (d, J=18Hz, O-PC($\underline{C}H_3)_3$).

$^{31}P\{^1H\}$ NMR (162 MHz, C_6D_6): δ 159.0 (s, O-P^{t}Bu$_2$), 78.2 (s, Ti-P^{t}Bu$_2$).

IR (solid state): 2950, 2896, 2865, 1573, 1556, 1426, 1402, 1366, 1271, 1228, 1198, 1183, 1041, 993, 807, 785, 697, 658, 624, 587, 542, 486, 468, 438

1.7 {(^{iPr}POCOP)TiCl$_3$}$_2$ (4)

^{iPr}POCOP-Li (Assumed 100% yield from previous step, 0.105 mmol, 1 equiv.) in pentane and cooled to −78 °C. $TiCl_4$ (12 µL, 0.109 mmol, 1 eqv) in pentane was added dropwise to the solution which immediately changed from colourless to brick red. The mixture was warmed to room temperature and stirred overnight. Solvents were removed *in vacuo* and the product extracted in hexane and filtered. Crystals suitable for x-ray diffraction were grown from a hexane solution at −40°C. Isolated crystalline yield 64 mg (0.129 mmol, 27% from ^{iPr}POCOP-Br)

^1H NMR (400 MHz, C_6D_6): δ 6.84 (t, 1H, *J*= 8 Hz $C_{aryl\text{-}para}$) 6.61 (d, 2H, *J*= 8 Hz $C_{aryl\text{-}meta}$), 2.65 (br, 4H, P($C\underline{H}(CH_3)_2)_2$), 1.17 (m, 24H, P(CH($C\underline{H}_3)_2)_2$).

^{31}P NMR (162 MHz, C_6D_6): δ 178.0.

^{13}C NMR (101 MHz, C_6D_6): δ 163.6 ($C_{aryl\text{-}ortho)}$, 132.2 ($C_{aryl\text{-}para}$), 108.5 ($C_{aryl\text{-}meta}$), 31.2 (P($\underline{C}H(CH_3)_2)_2$), 17.1 (P(CH($\underline{C}H_3)_2)_2$), 16.8 (P(CH($\underline{C}H_3)_2)_2$). Resonances for $C_{aryl\text{-}ipso}$ not observed.

1.8 (^{tBu}POCOP)TiMe$_2$ (5)

(^{tBu}POCOP)$TiCl_2$ (200 mg, 0.39 mmol, 1 equiv.) was dissolved in toluene and MeMgCl (3 M in THF, 0.27 mL, 2.1 equiv.) was added. The mixture was stirred at room temperature for 3 hours and the bright blue solution changed to a dark teal solution. 1,4-Dioxane (~2 mL) was added and the mixture allowed to stir for 30 mins. The mixture was filtered and solvents removed *in vacuo,* to yield a teal residue. The product was extracted in pentane, concentrated and crystallised at −40 °C, yielding (^{tBu}POCOP)$TiMe_2$ (94 mg, 51%).

Elemental Analysis found (calculated for $C_{24}H_{45}O_2P_2Ti$): C 56.33 (60.63), H 8.42 (9.54). *Accurate elemental analysis could not be achieved due to air-sensitive and phosphorus containing nature of sample.*

^1H NMR (400 MHz,C_6D_6): δ 8.72 (s, 1H), 5.66 (s, 2H), 3.87 (s, 42H).

$^{31}P\{^1H\}$ NMR (162 MHz, C_6D_6): No resonances observed.

μ_{eff} (Evan's method): 2.03 μ_B

X Band CW EPR (300 K, toluene): g_{iso}: 1.970, Hyperfine coupling to two ^{31}P nuclei (a_0 = 2.25 mT) and super hyperfine coupling to six ^1H nuclei (a_0 =0.64 mT).

IR (solid state): 2957, 2898, 2865, 1569, 1546, 1470, 1410, 1389, 1365, 1265, 1216, 1179, 1109, 1078, 1021, 963, 932, 865, 807, 773, 714, 702, 619, 566, 495, 468, 451, 429.

1.9 (^{tBu}POCOP)TiPhCl (6)

(^{tBu}POCOP)$TiCl_2$ (250 mg, 0.48 mmol, 1 equiv.) was dissolved in toluene and PhMgCl in THF (2M, 0.26 mL, 1.1 equiv) added at room temperature. Solution immediately changes from a blue solution to a green solution and the mixture was allowed to stir at room temperature for 2 hours. 1,4-Dioxane was added and the mixture filtered through celite. Solvents were removed in vacuo and the product extracted in pentane and filtered. (^{tBu}POCOP)TiPhCl was isolated by cooling a saturated pentane solution to −40°C as dark green blocks (105 mg, 39%).

On one occasion PhMgBr was used in place of PhMgCl and this resulted in (^{tBu}POCOP)TiPhBr being isolated as a single crystals sample.

Elemental Analysis found (calculated for $C_{28}H_{44}Cl_1O_2P_2Ti$): C 58.97 (60.28), H 7.62 (7.95). *Accurate elemental analysis could not be achieved due to air-sensitive and phosphorus containing nature of sample.*

^{1}H NMR (400 MHz, C_6D_6): δ 9.61 (br), 4.27 (s), 3.78 (br), 2.05 (br), 0.88 (s).

^{31}P{^{1}H} NMR (162 MHz, C_6D_6): No resonances observed.

μ_{eff} (Evan's method): 2.08 μ_B

X Band CW EPR (299 K, toluene): Major: 60%. g_{iso}: 1.9665, hyperfine coupling to two ^{31}P nuclei (a_0 = 2.26 mT). Minor: 40% g_{iso}: 1.972, hyperfine coupling to two ^{31}P nuclei (a_0 = 2.24 mT)

IR (solid state): 3042, 2945, 2896, 2864, 1571, 1547, 1645, 1413, 1390, 1366, 1178, 1077, 1022, 1009, 965, 870, 820, 807, 716, 701, 617, 481, 452, 436.

1.10 (^{tBu}POCOP)TiNpCl (7)

(^{tBu}POCOP)$TiCl_2$ (250 mg, 0.48 mmol, 1 equiv.) was dissolved in pentane and a pentane solution of neopentyl lithium (38 mg, 0.48 mmol, 1 equiv) was added at −78°C. The solution was allowed to warm to room temperature and stirred for 1 hour, with the blue solution turning green. Solvents were then removed *in vacuo*. The product was extracted in pentane and filtered through celite. Crystals suitable for x-ray diffraction were grown from cooling a saturated pentane solution to −40°C. (^{tBu}POCOP)TiNpCl was isolated as dark green blocks (165 mg, 63%).

Elemental Analysis found (calculated for $C_{27}H_{50}Cl_1O_2P_2Ti$): C 57.99 (58.75), H 9.13 (8.96). *Accurate elemental analysis could not be achieved due to air-sensitive and phosphorus containing nature of sample.*

^{1}H NMR (400 MHz, C_6D_6): δ 11.81 (br, 2H), 7.62 (s, 1H), 3.34-2.53 (br d, 36H), 1.50 (d, 1H), 1.17 (d, 1H), -0.40 (br, 9H).

^{31}P{^{1}H} NMR (162 MHz, C_6D_6): No resonances observed.

μ_{eff} (Evan's method): 1.75 μ_B

X Band CW EPR (304 K, toluene): Major: 90%. g_{iso}: 1.9665, hyperfine coupling to two ^{31}P nuclei (a_0 = 2.20 mT). Minor: 10% g_{iso}: 1.9709, hyperfine coupling to two ^{31}P nuclei (a_0 = 2.20 mT).

IR (solid state): 2945, 2897, 2865, 1579, 1546, 1469, 1413, 1392, 1365, 1216, 1181, 1146, 1020, 964, 934, 866, 811, 779, 705, 625, 484, 457, 404.

1.11 {(^{tBu}POCOP)TiHCl}$_2$ (8)

Method 1: Crystals of (^{tBu}POCOP)TiNpCl (25 mg, 0.05 mmol) were exposed to an atmosphere of H_2 (1.8 bar). Green crystals immediately turn dark purple/black. The product was dissolved in the minimal amount of tetramethylsilane, filtered through celite and crystallised at −40 °C. Yield 23 mg (0.023 mmol) 95%

Method 2: (^{tBu}POCOP)TiNpCl was dissolved in pentane. The solution was degassed with one cycle of freeze-pump-thaw. The frozen solution under vacuum, H_2 (1 bar) was added. The mixture was allowed to warm up to 0°C, with the green solution changing to a dark purple solution. Yield is quantitative.

^{1}H NMR (400 MHz, d_8-tol): δ 12.09 (s), 7.65 (s), 6.71 (s), 6.63 (s), 3.42-2.58 (br d), 2.27 (s), 1.87 (s), 1.17 (d),1.09 (s), 0.91 (s, C(CH_3)$_4$), 0.75 (d), -0.52 (br).

^{31}P{^{1}H} NMR (162 MHz, C_6D_6): No resonances observed.

μ_{eff} (Evan's method): 3.37 μ_B

X Band CW EPR (304 K, toluene): Major: 90%. g_{iso}: 1.9665, hyperfine coupling to two ^{31}P nuclei (a_0 = 2.20 mT). Minor: 10% g_{iso}: 1.9736, hyperfine coupling to two ^{31}P nuclei, hyperfine coupling to 1 ^{1}H nucei (a_0 = 2.24 mT and a_0 = 0.642)

IR (solid state): 2949, 2895, 2864, 1577, 1545, 1469, 1413, 1391, 1363, 1262, 1215, 1178, 1126, 1077, 1021, 964, 867, 809, 773, 715, 701, 627, 611, 585, 483, 457.

2. Crystallography Data Tables

	Li^{tBu}POCOP	2	3	4
Crystal Data				
Chemical formula	$C_{22}H_{39}LiO_2P_2$	$C_{22}H_{39}Cl_3O_2P_2Ti$	$C_{44}H_{78}Cl_2O_4P_4Ti$ (+ solvent)	$C_{36}H_{62}Cl_6O_4P_4Ti_2$
M_r	404.44	551.76	609.2	991.3
Crystal system, space group	Orthorhombic, $Pna2_1$	Monoclinic, $P2_1$	Monoclinic, $P2_1/c$	Monoclinic, $P2_1/c$
***a*, *b*, *c* (Å)**	21.9510 (7), 14.8413 (5), 15.1618 (4)	9.8749 (2), 10.5591 (3), 13.2857 (3)	19.8638 (10), 29.354 (2), 19.5939 (11)	11.9525 (3), 13.0318 (2), 15.1944 (4)
a, b, γ (°)	90, 90, 90	90, 99.419 (2), 90	90, 96.659 (5), 90	90, 101.440 (2), 90
***V* (Å^3)**	4939.4 (3)	1366.62 (6)	11347.8 (12)	2319.70 (9)
Z	8	2	12	2
Radiation type	Cu K_α	Cu K_α	Cu K_α	Cu K_α
μ (mm^{-1})	1.68	6.58	3.46	7.7
Crystal size (mm)	0.10 × 0.10 × 0.05	0.10 × 0.10 × 0.05	0.10 × 0.10 × 0.05	0.05 × 0.05 × 0.05
Data Collection				
T_{min}, T_{max}	0.83, 0.85	0.59, 0.72	0.44, 0.84	0.30, 0.68
No. of measured, independent and observed [I > 2.0s(I)] reflections	10545, 7239, 5360	4812, 3568, 3251	37934, 21794, 5778	13979, 4544, 3840
R_{int}	0.063	0.049	0.172	0.042
Refinement				
R_1 [I > 2σ(I)]	0.066	0.050	0.118	0.058
wR_2 [I > 2σ(I)]	0.162	0.136	0.46	0.173
GooF	0.99	1.01	1.45	1.53
No. of reflections	7239	3568	21794	4544
No. of parameters	487	272	991	235
No. of restraints	1	418	0	0
Residual Electron Density (e Å^{-3})	0.51, -0.42	0.62, -0.41	2.16, -2.53	1.15, -0.87
Absolute structure	Parsons, Flack & Wagner (2013), 1945 Friedel Pairs	Parsons, Flack & Wagner (2013), 784 Friedel Pairs	–	–
Absolute structure parameter	-0.00 (4)	-0.033(14)	–	–
CCDC	2204753	2204754	2204755	2204756

	5	6	6B	7	8
Crystal data					
Chemical formula	$C_{24}H_{45}O_2P_2Ti$	$C_{28}H_{44}ClO_2P_2Ti$	$C_{28}H_{44}BrO_2P_2Ti$	$C_{27}H_{50}ClO_2P_2Ti$	$C_{26}H_{52}ClO_2P_2SiTi$
M_r	475.47	557.96	602.41	551.99	570.08
Crystal system, space group	Monoclinic, $P2_1/n$	Monoclinic, $P2_1/n$	Monoclinic, $P2_1/n$	Tetragonal, $P\bar{4}2_1c$	Monoclinic, $P2_1/c$
***a*, *b*, *c* (Å)**	14.0280 (2), 12.6260 (3), 15.6016 (3)	15.3936 (3), 12.7200 (3), 15.5084 (4)	15.4564 (2), 12.7270 (2), 15.5888 (2)	17.1600 (3), 17.1600 (3), 21.1327 (5)	10.7943 (1), 22.1846 (3), 27.3239 (3)
a, b, γ (°)	90, 90.8481 (16), 90	90, 98.601 (2), 90	90, 97.7926 (14), 90	90, 90, 90	90, 91.8675 (10), 90
***V* (Å^3)**	2763.01 (9)	3002.50 (12)	3038.21 (7)	6222.9 (3)	6539.70 (13)
Z	4	4	4	8	8
Radiation type	Cu K_α	Mo K_α	Cu K_α	Cu K_α	Cu K_α
μ (mm^{-1})	3.83	0.5	5.08	4.24	4.39
Crystal size (mm)	0.30 × 0.20 × 0.10	0.50 × 0.20 × 0.05	0.30 × 0.30 × 0.10	0.20 × 0.20 × 0.20	0.30 × 0.20 × 0.10
Data collection					
T_{min}, T_{max}	0.49, 0.68	0.69, 0.98	0.50, 0.60	0.37, 0.43	0.18, 0.64
No. of measured, independent and observed [I > 2.0s(I)] reflections	8480, 5250, 4260	41186, 6774, 5162	10033, 5799, 4303	11746, 3386, 3092	21714, 12534, 9694
R_{int}	0.034	0.050	0.042	0.036	0.044
Refinement					
R_1 [I > 2σ(I)]	0.042	0.041	0.046	0.058	0.073
wR_2 [I > 2σ(I)]	0.057	0.095	0.112	0.159	0.195
GooF	1.04	1.02	0.91	0.91	0.98
No. of reflections	5248	6768	5799	3386	12534
No. of parameters	262	307	307	299	596
No. of restraints	425	472	799	0	0
Residual Electron Density (e Å^{-3})	0.58, -0.65	0.55, -0.55	0.67, -0.90	1.42, -0.36	3.23, -0.74
Absolute structure	–	–	–	Parsons, Flack & Wagner (2013), 0 Friedel Pairs	–
Absolute structure parameter	–	–	–	0	–
CCDC	2204757	2204758	2204759	2204760	2204761

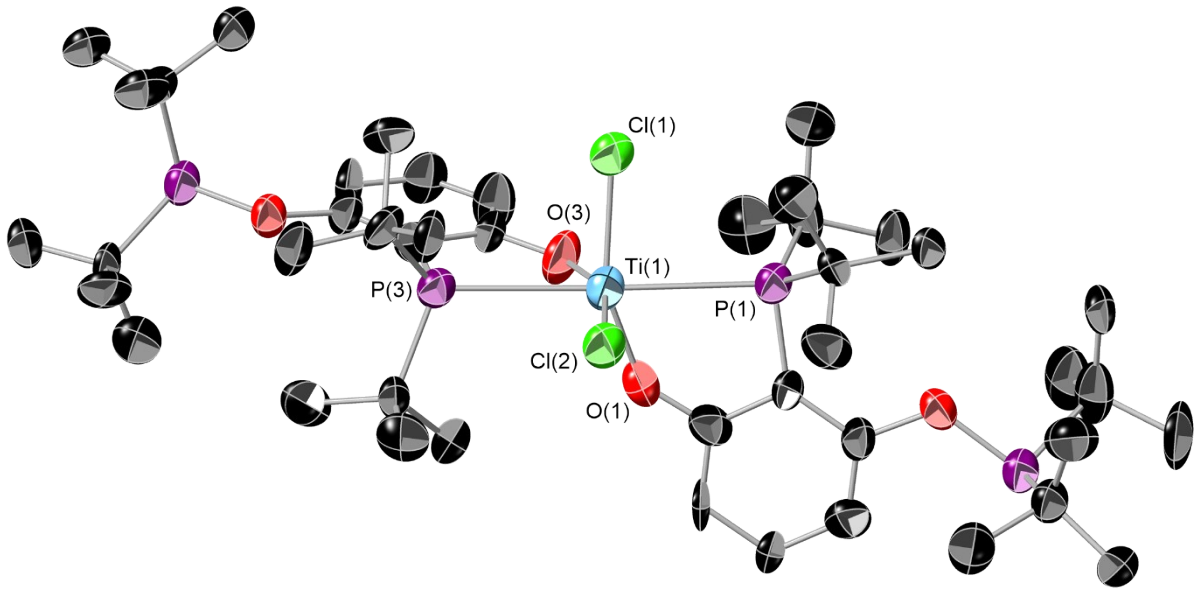

Figure S1: *ORTEP plot of **3**. Thermal ellipsoids at 50% probability, hydrogens omitted for clarity. Colour key: sky blue (titanium), black (carbon); purple (phosphorus), red (oxygen), green (chlorine). Selected bond angles (°): P(1)-Ti(1)-P(3) 178.4(2), P(1)-Ti(1)-O(1) 71.3(4), Cl(1)-Ti(1)-Cl(2) 95.3(2), O(1)-Ti(1)-O(3) 89.5(6).*

3. EPR Spectra

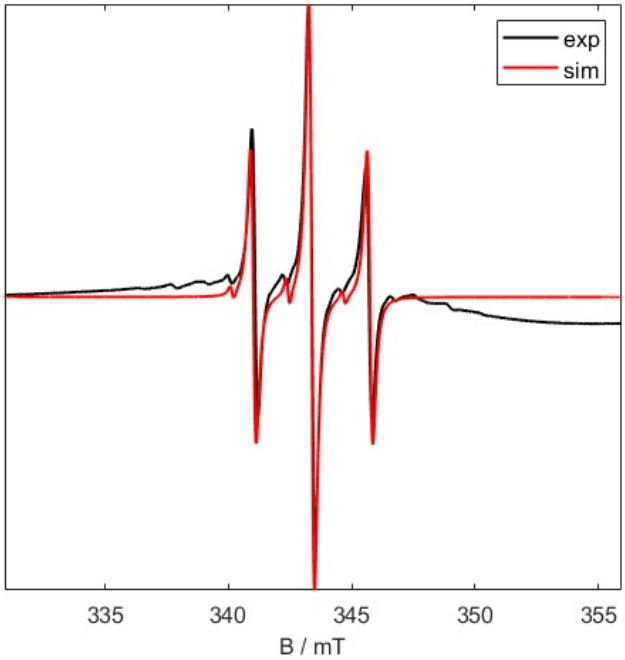

Figure S2: *X Band CW EPR of **1** in toluene (303 K). Experimental data (black) and simulated spectra (red).*

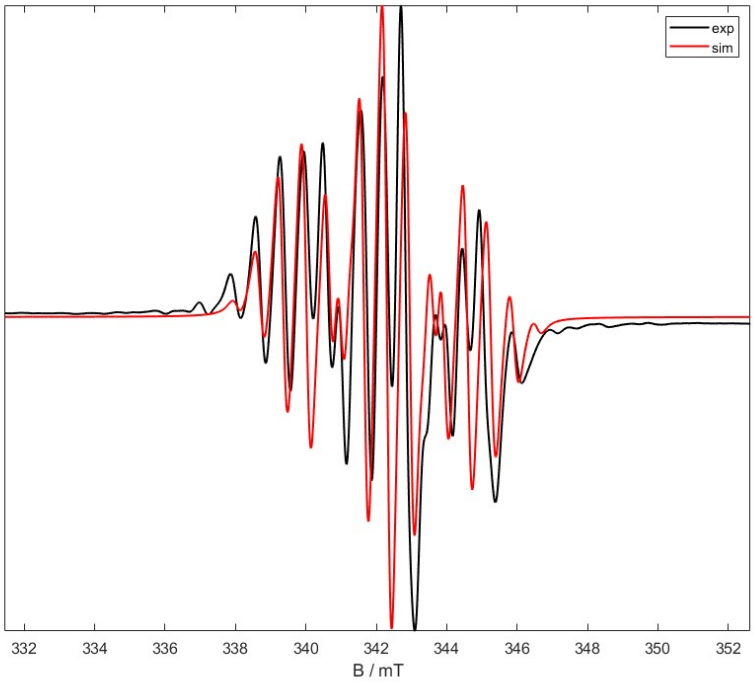

***Figure S3**: X Band CW EPR of **5** in toluene (300 K). Experimental data (black) and simulated spectra (red).*

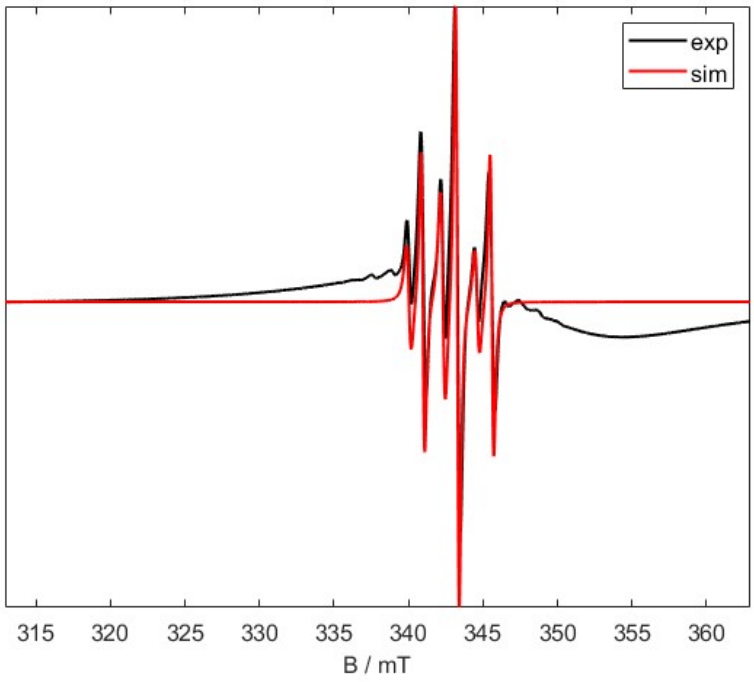

***Figure S4:** X Band CW EPR of **6** in toluene (299 K). Experimental data (black) and simulated spectra (red).*

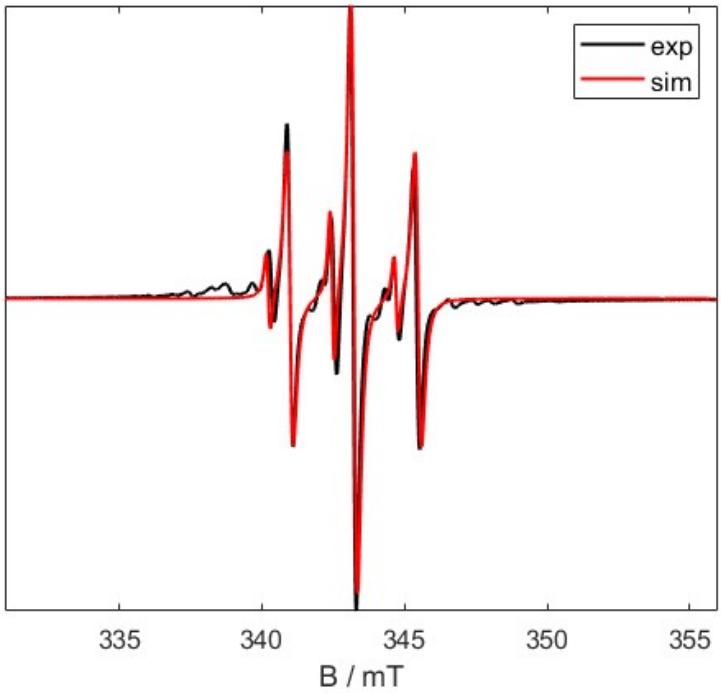

Figure S5: *X Band CW EPR of **7** in toluene (304 K). Experimental data (black) and simulated spectra (red).*

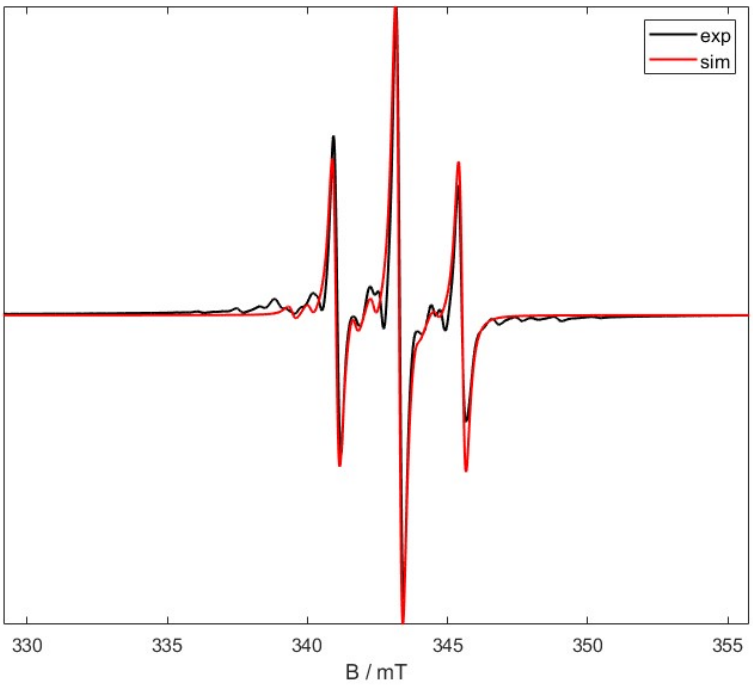

Figure S6*: X Band CW EPR of **8** in toluene (304 K). Experimental data (black) and simulated spectra (red).*

4. IR Spectra

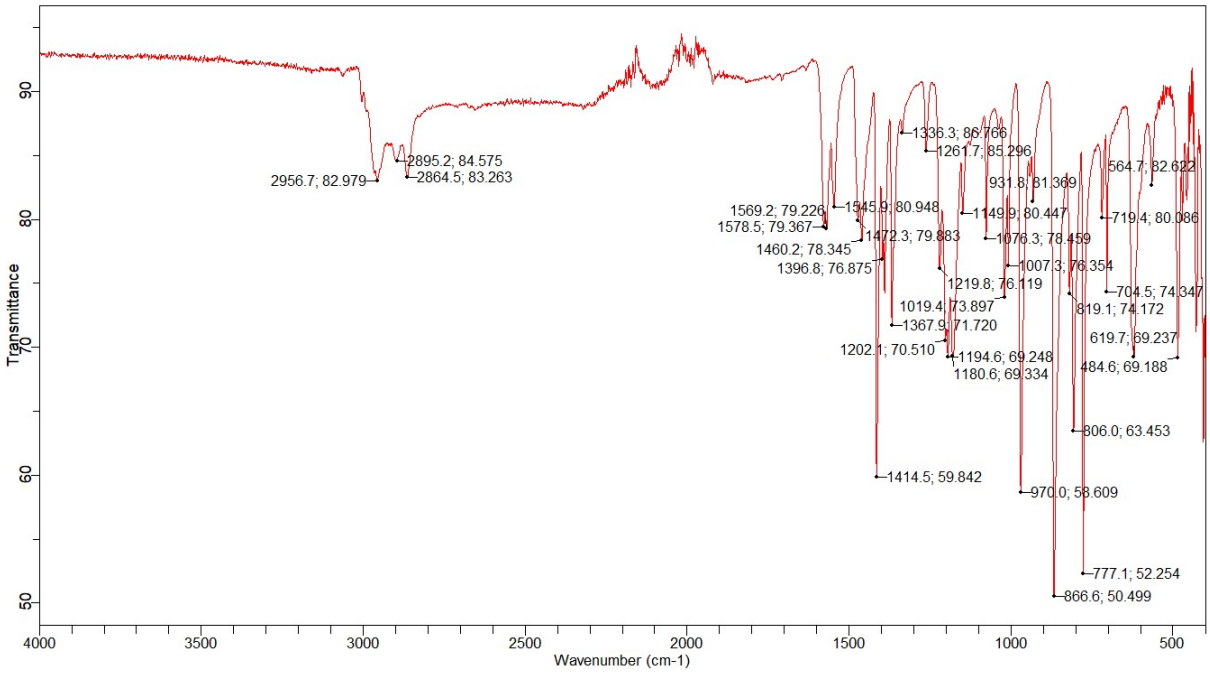

Figure S7: *IR Spectra for* ***1****.*

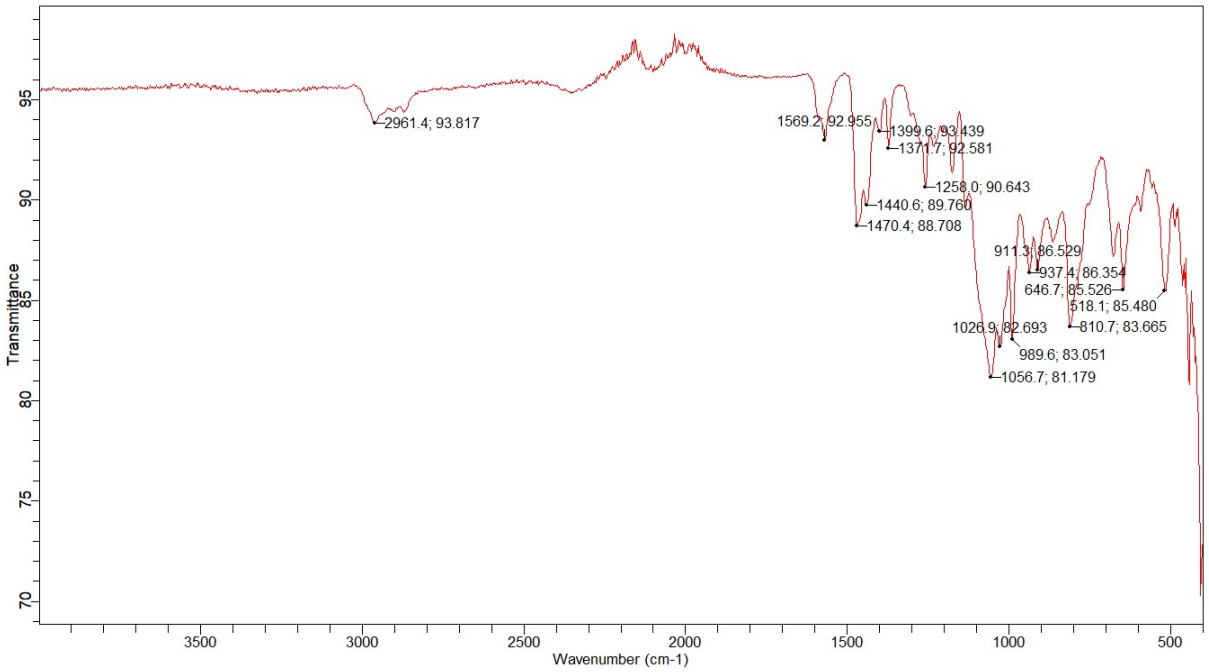

Figure S8: *IR Spectrum of* ***2****.*

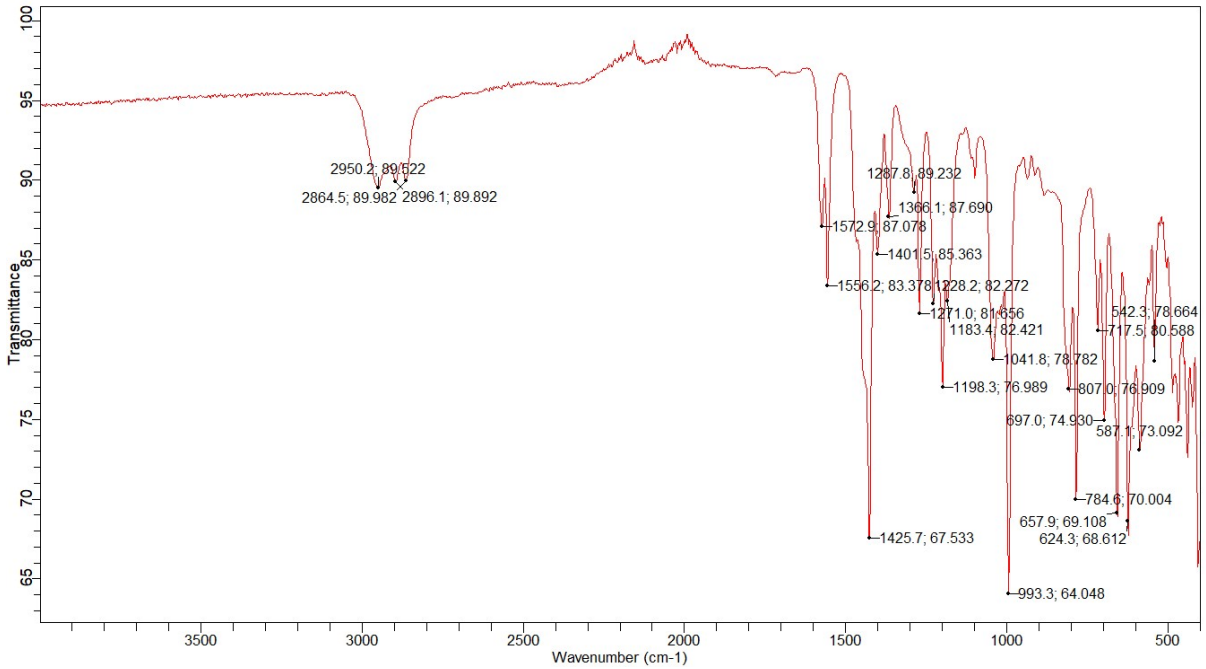

Figure S9: *IR Spectra of* ***3****.*

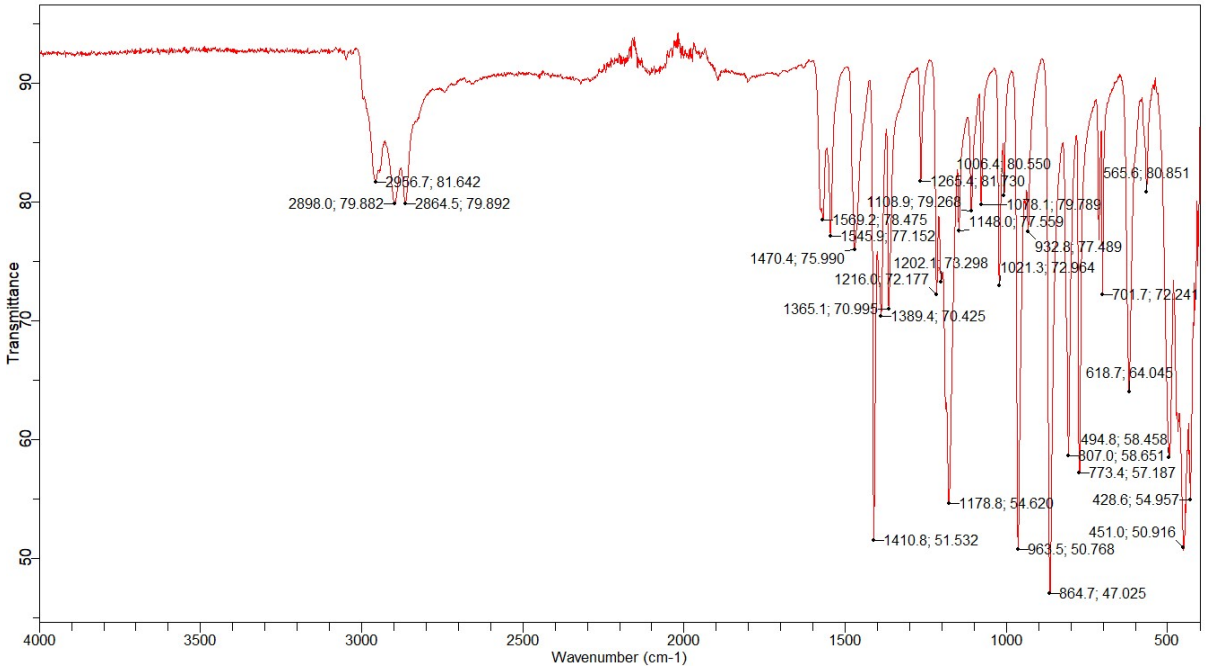

Figure S10: *IR Spectra for* ***5****.*

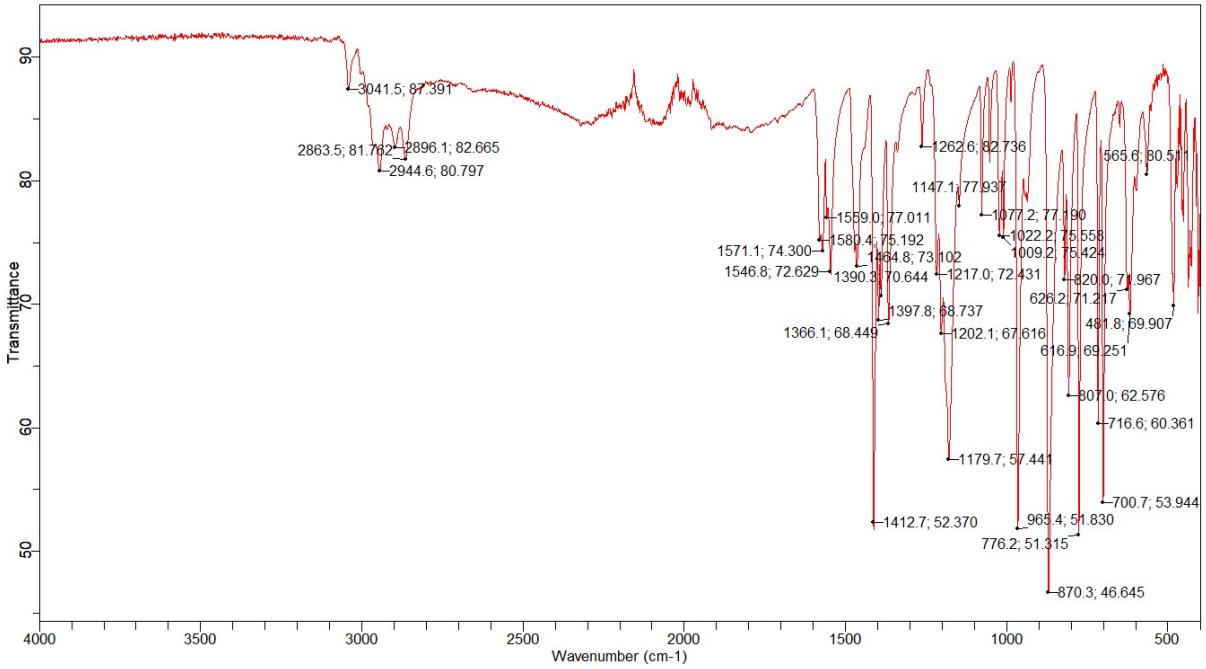

Figure S11: *IR Spectra for* ***6****.*

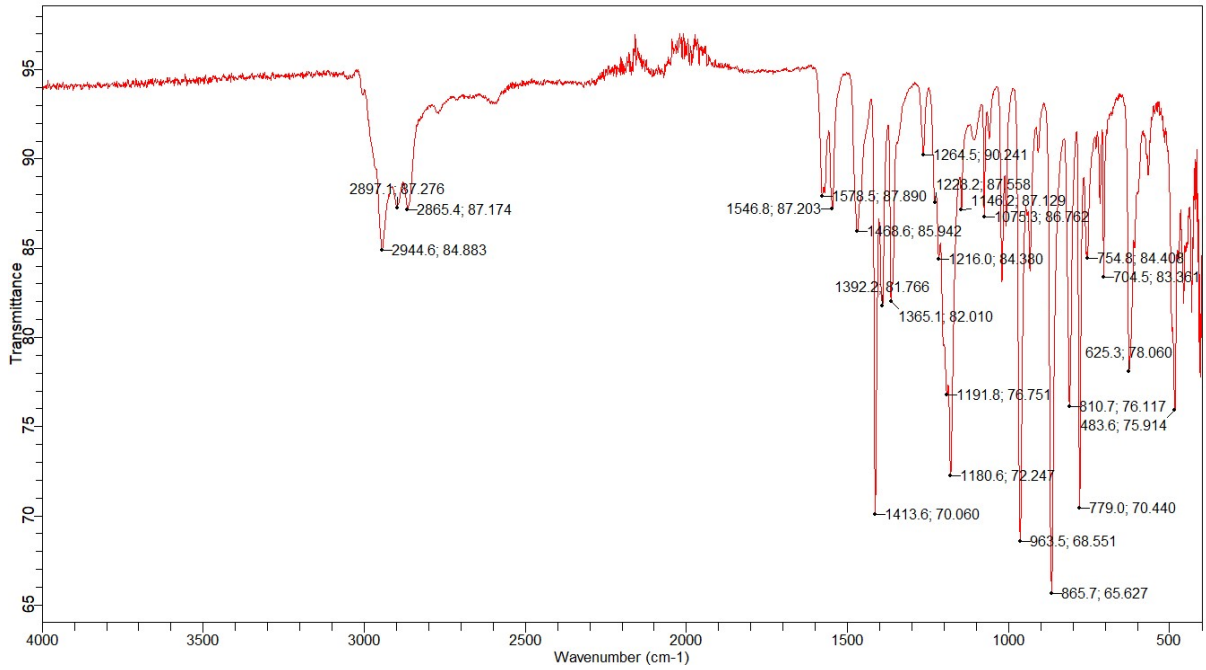

Figure S12: *IR Spectra for* ***7.***

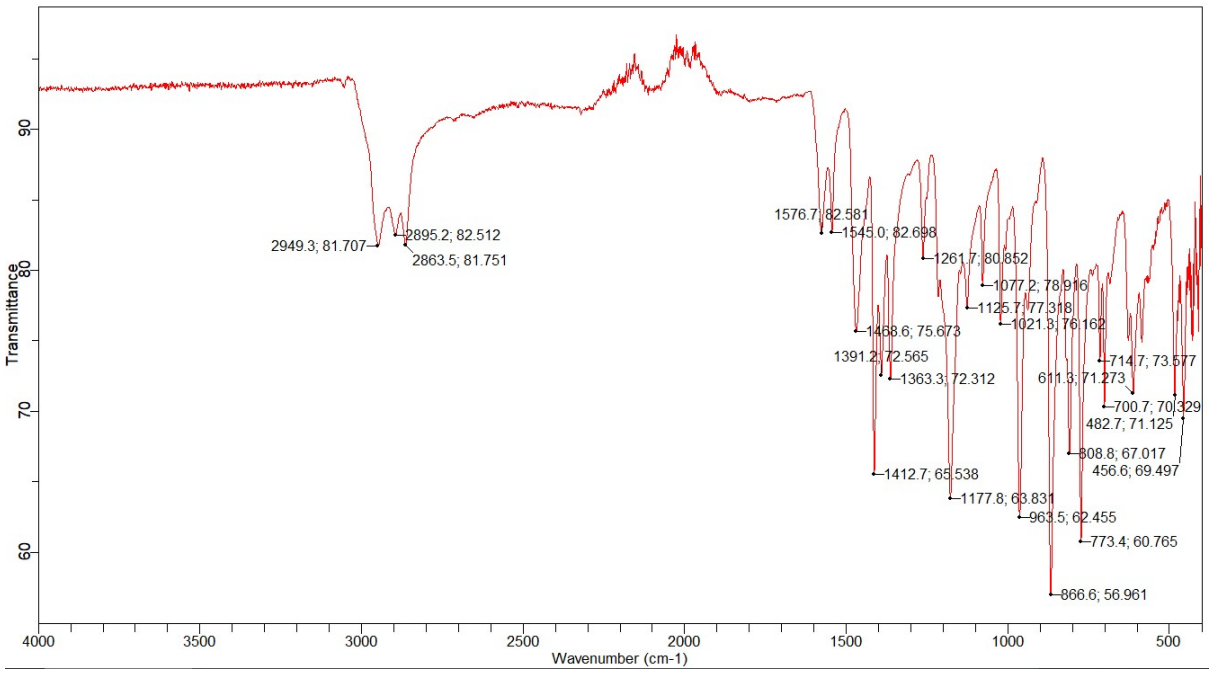

Figure S13: *IR Spectra for* ***8****.*

5. NMR

5.1 ^{tBu}POCOP-Li

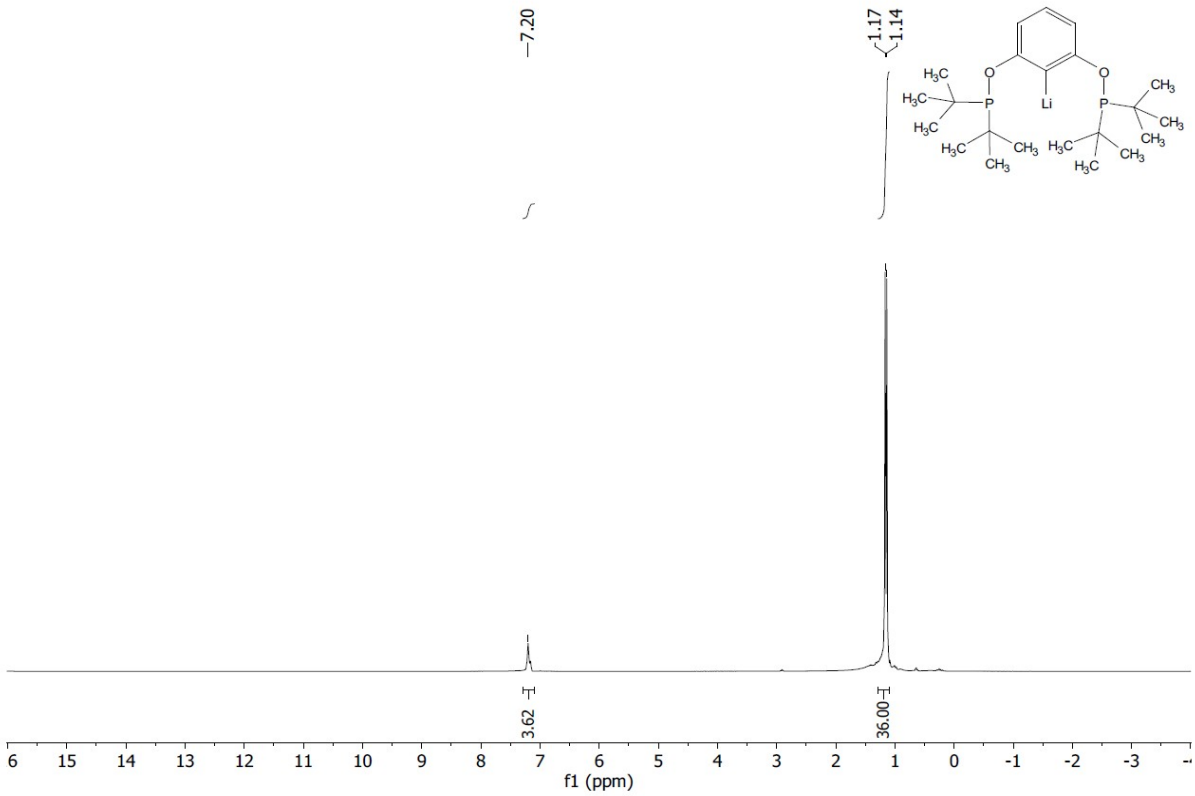

Figure S14: *^{1}H NMR (400 MHz, C_6D_6) of ^{tBu}POCOP-Li.*

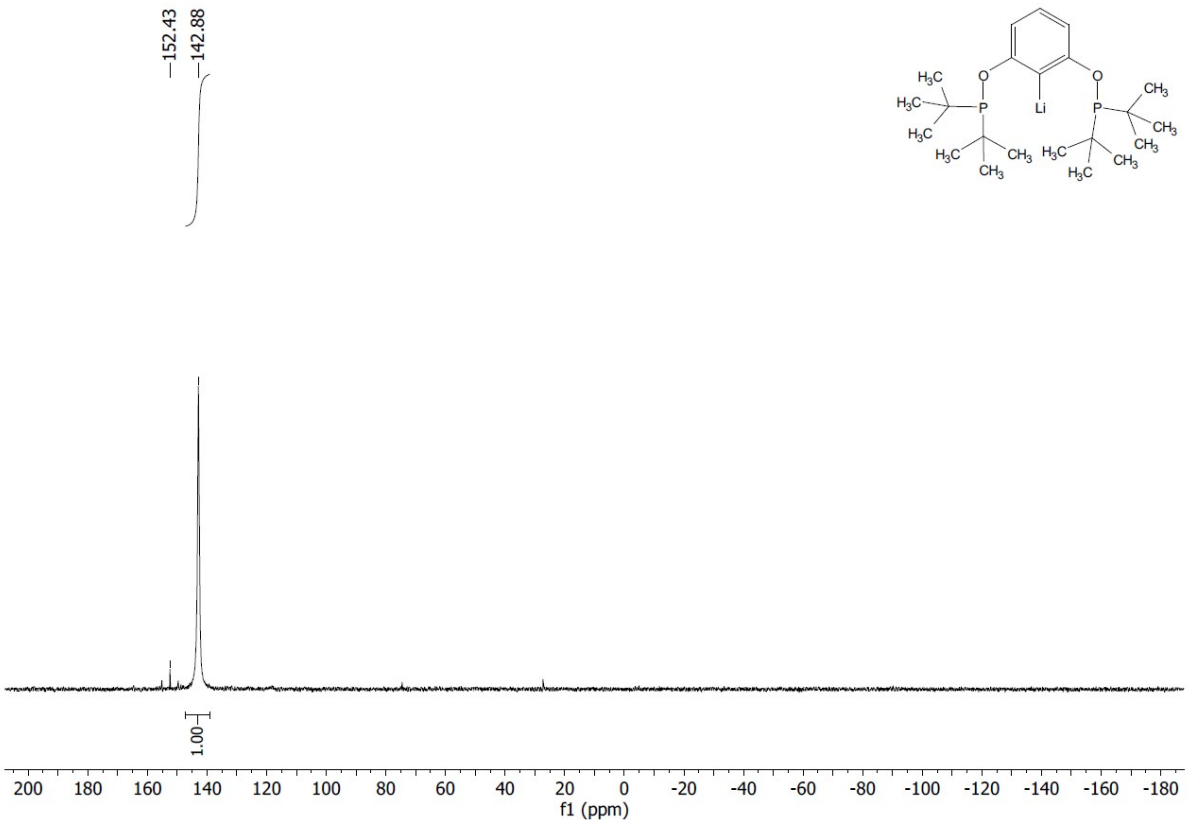

Figure S15: *^{31}P{^{1}H} NMR (162 MHz, C_6D_6) of ^{tBu}POCOP-Li.*

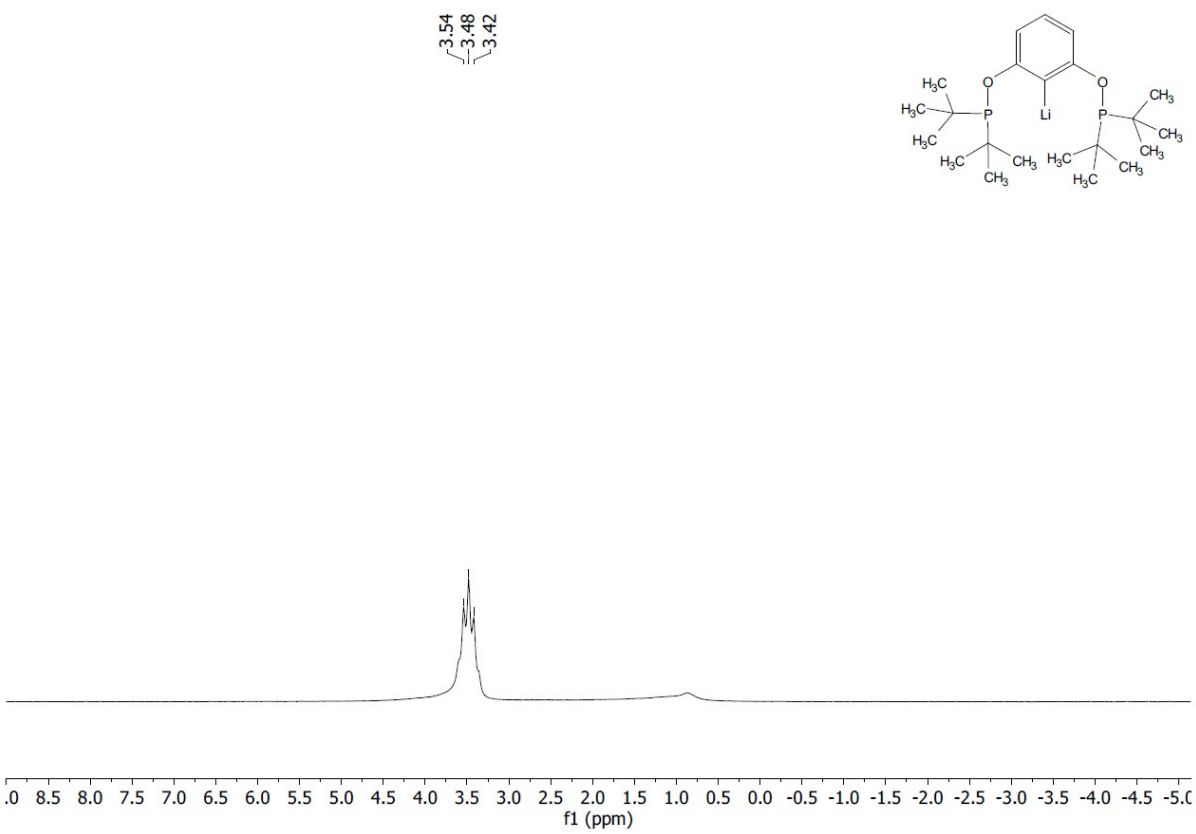

Figure S16: *^{7}Li NMR (156 MHz, C_6D_6) of ^{tBu}POCOP-Li.*

5.2 ^{iPr}POCOP-Li

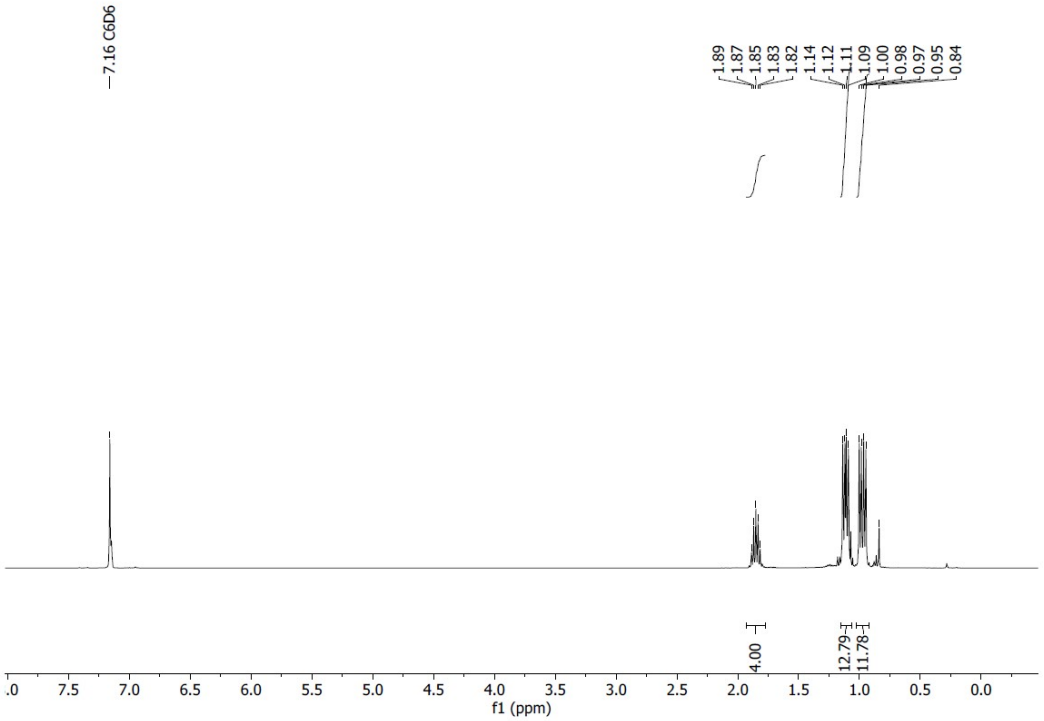

Figure S17: *^{1}H NMR (400 MHz, C_6D_6) of ^{iPr}POCOP-Li.*

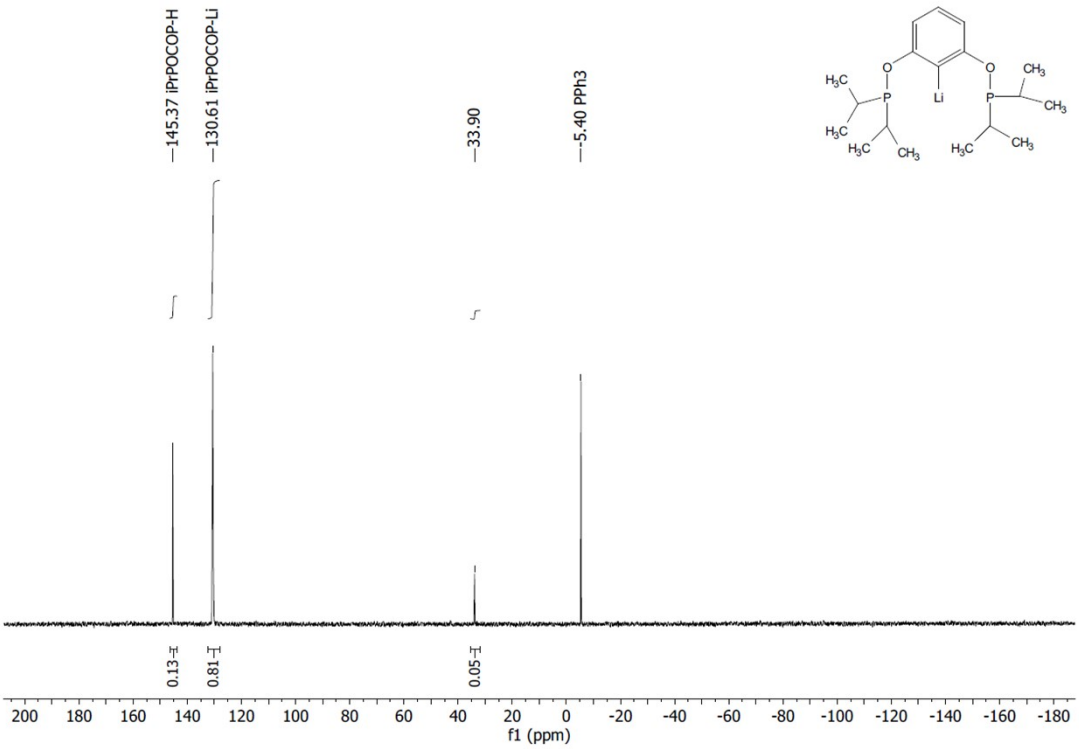

Figure S18: *^{31}P{^{1}H} NMR (162 MHz, C_6D_6) of ^{iPr}POCOP-Li.*

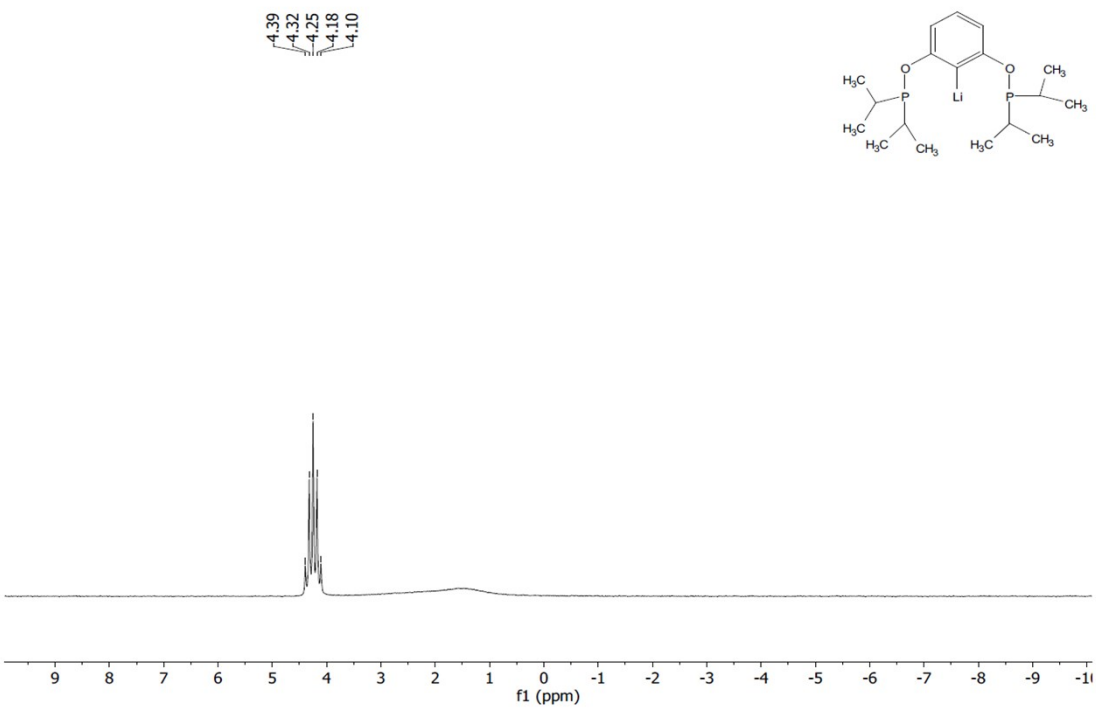

Figure S19: *^{7}Li NMR (156 MHz, C_6D_6) of ^{tBu}POCOP-Li.*

5.3 (^{tBu}POCOP)$TiCl_2$ (1)

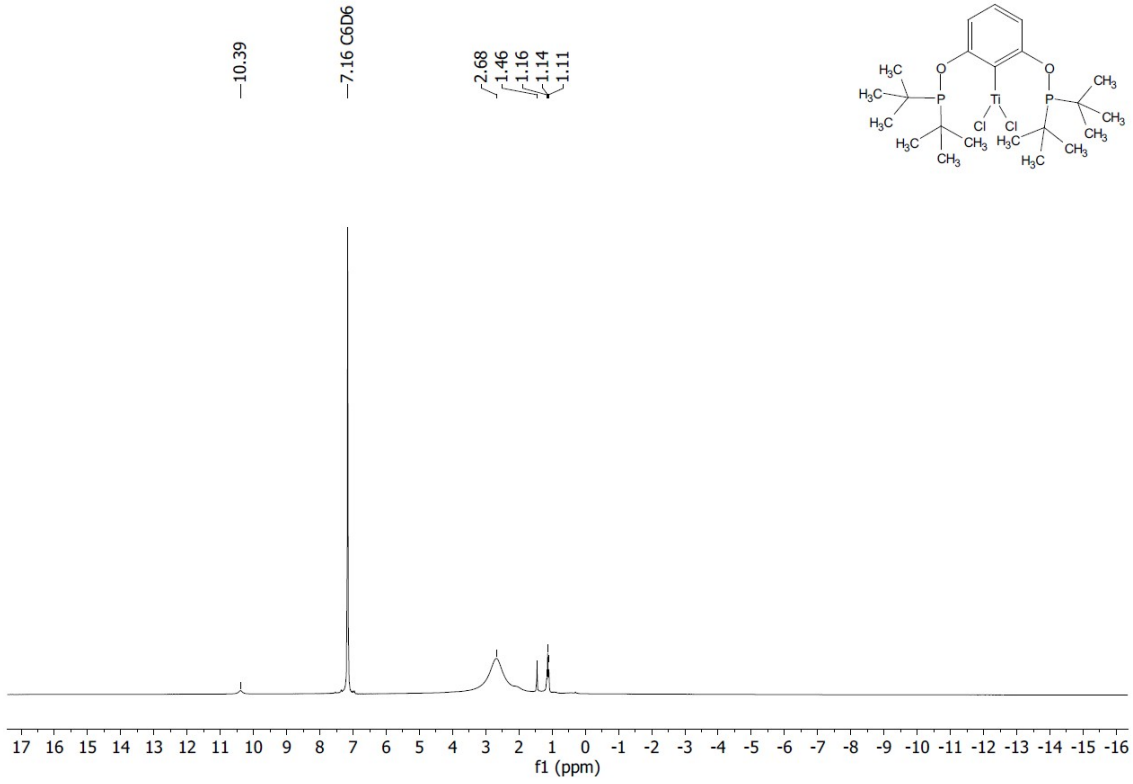

Figure S20: *^{1}H NMR (400 MHz, C_6D_6) of **1**.*

5.4 (^{tBu}POCOP)$TiCl_3$ (2)

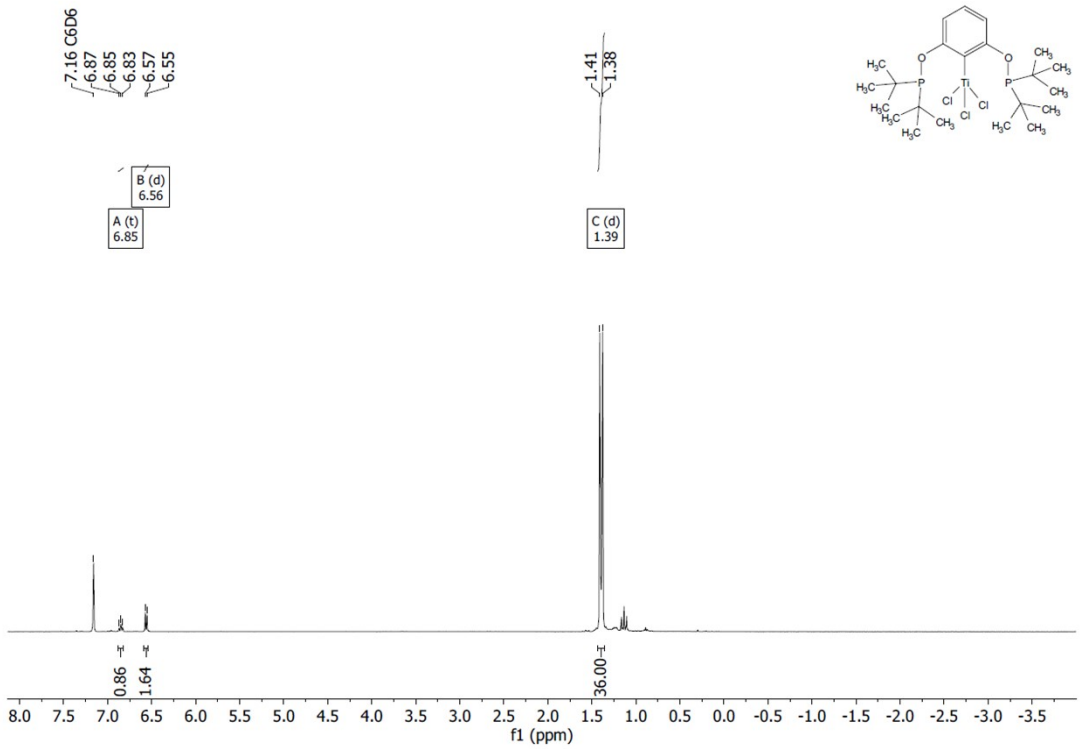

Figure S21: *^{1}H NMR (400 MHz, C_6D_6) of* ***2.***

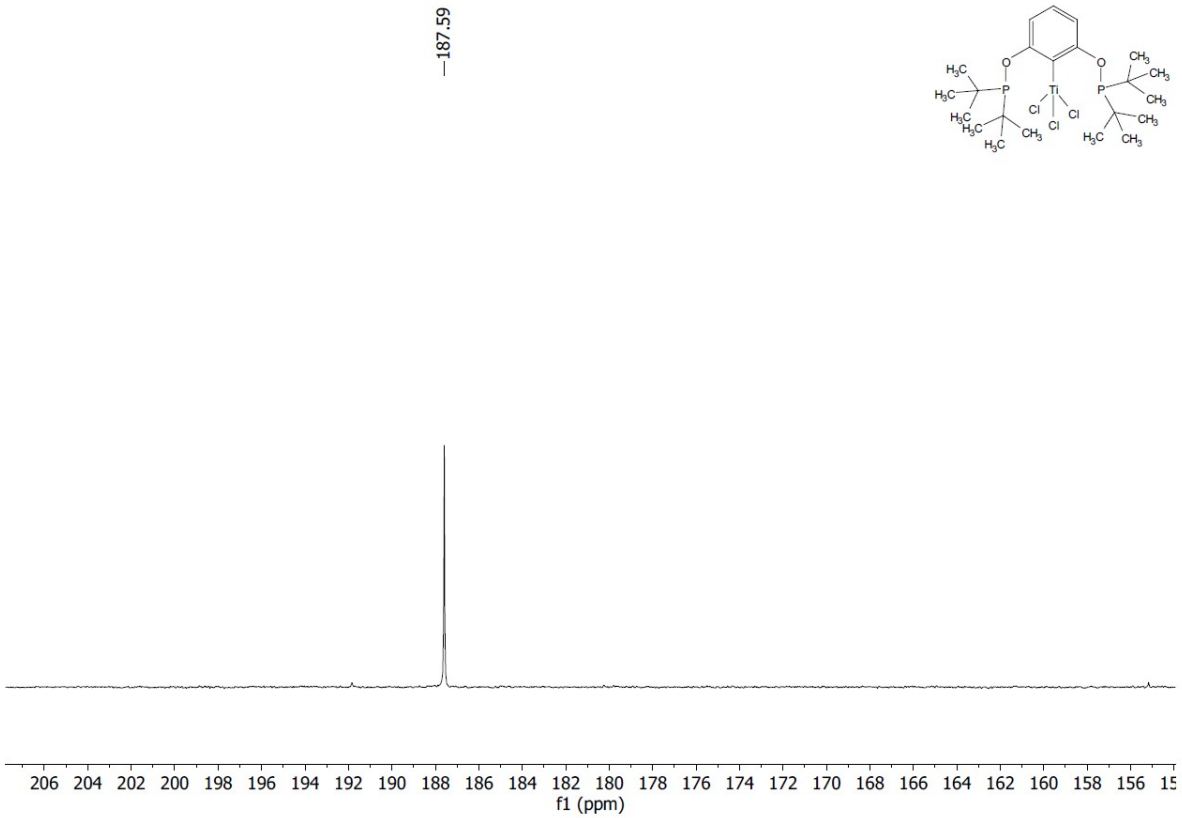

Figure S22: *$^{31}P\{^{1}H\}$ NMR (162 MHz, C_6D_6) of* ***2.***

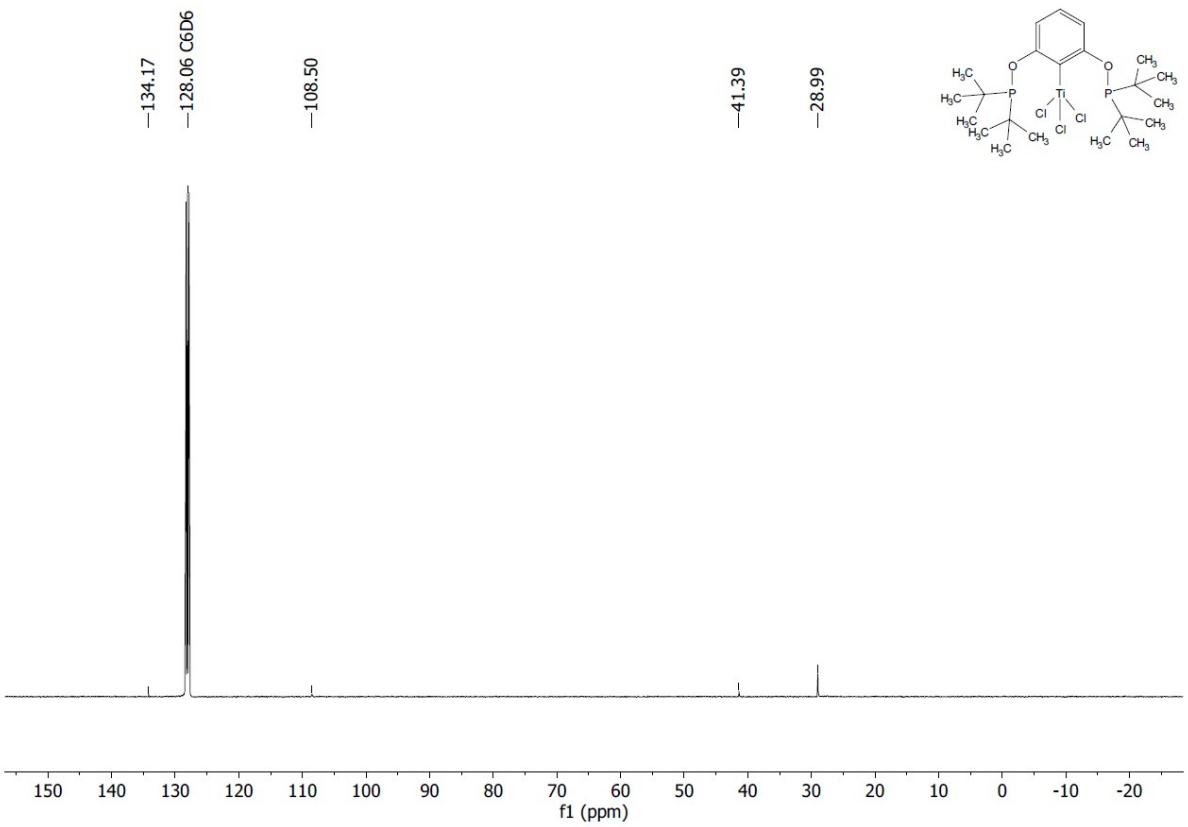

Figure S23: *^{13}C NMR (101 MHz, C_6D_6) of* ***2****.*

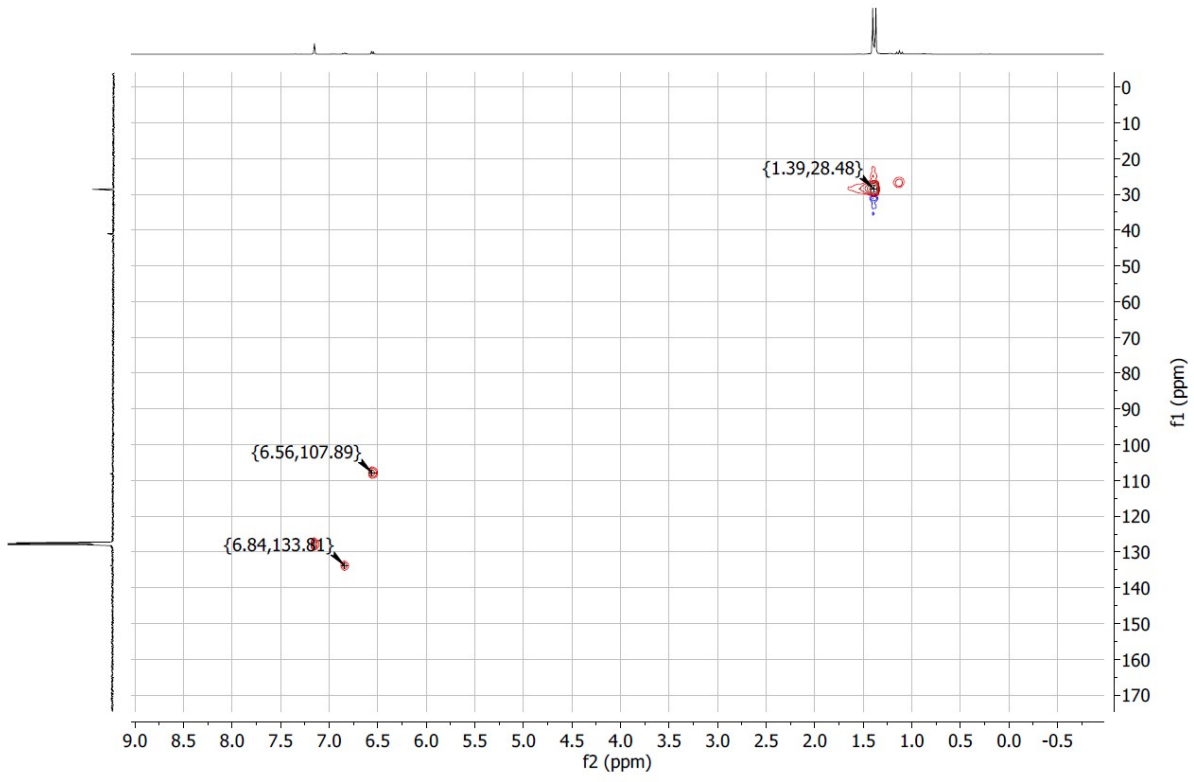

Figure S24: *HSQC NMR (C_6D_6) of* ***2****.*

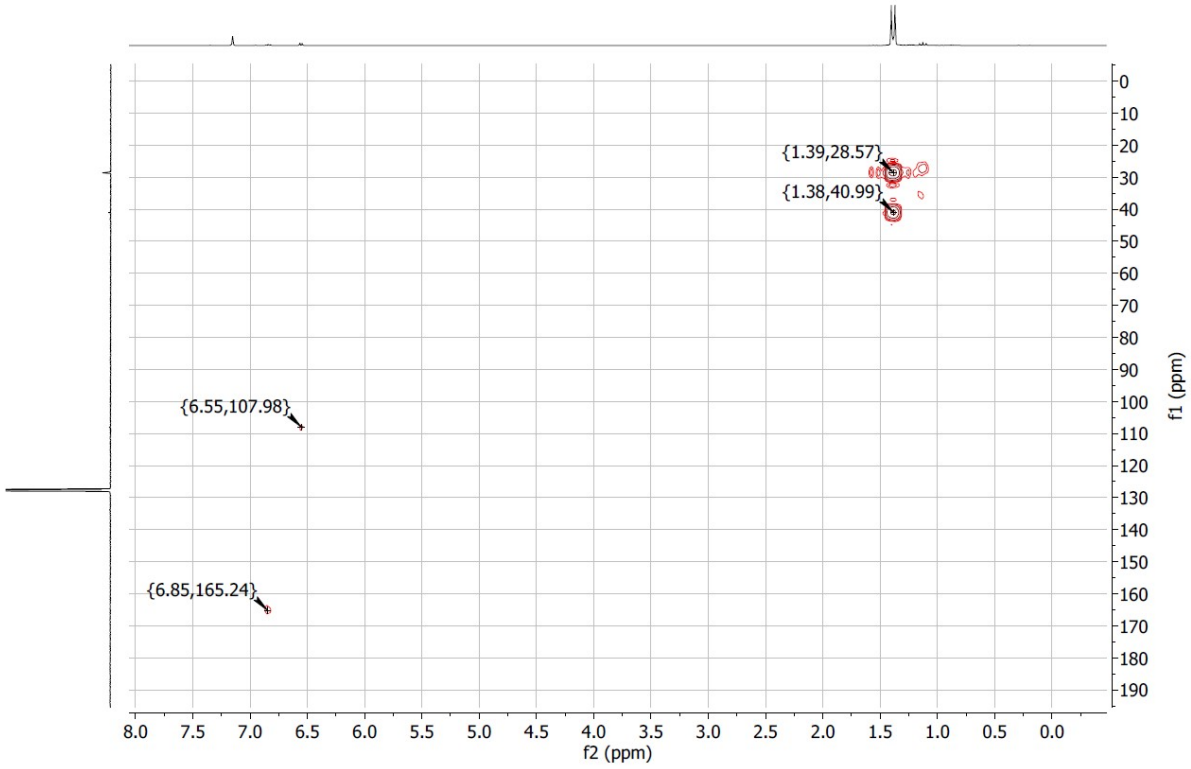

Figure S25: *HMBC NMR (C_6D_6) of* ***2.***

5.5 (^{tBu}POCOP*)$_2$TiCl$_2$ (3)

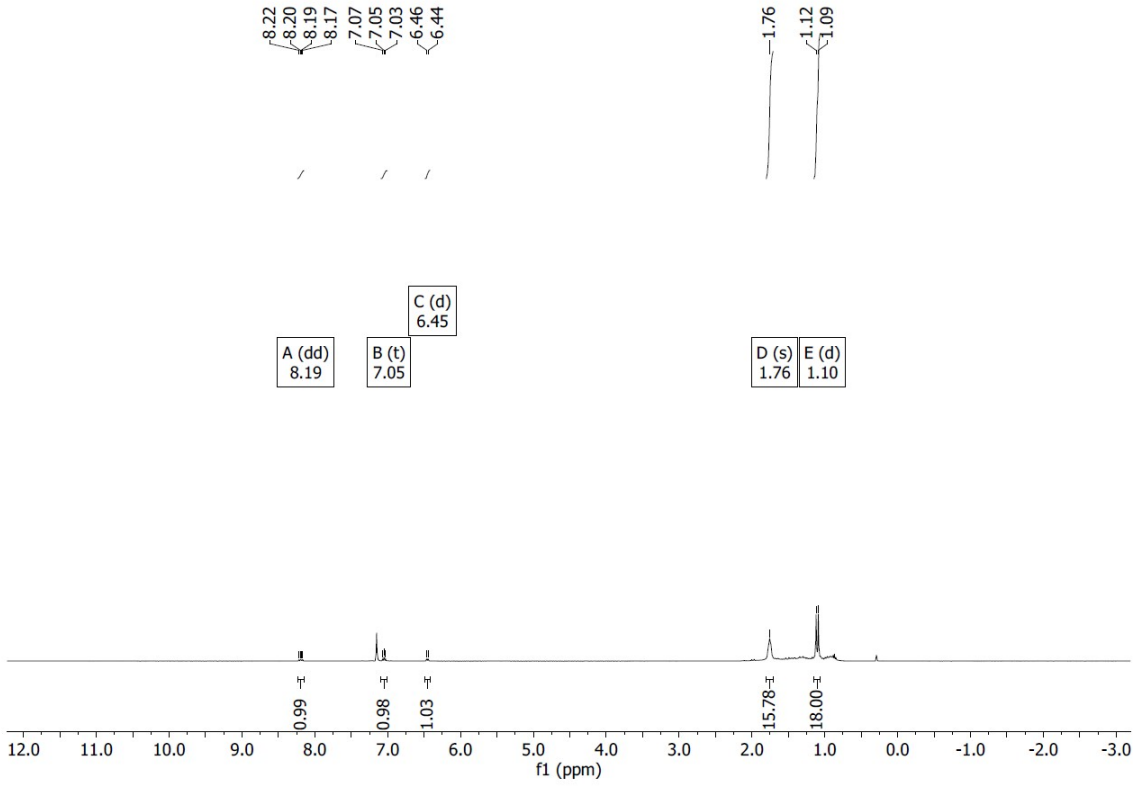

Figure S26: *^{1}H NMR (400 MHz, C_6D_6) of* ***3.***

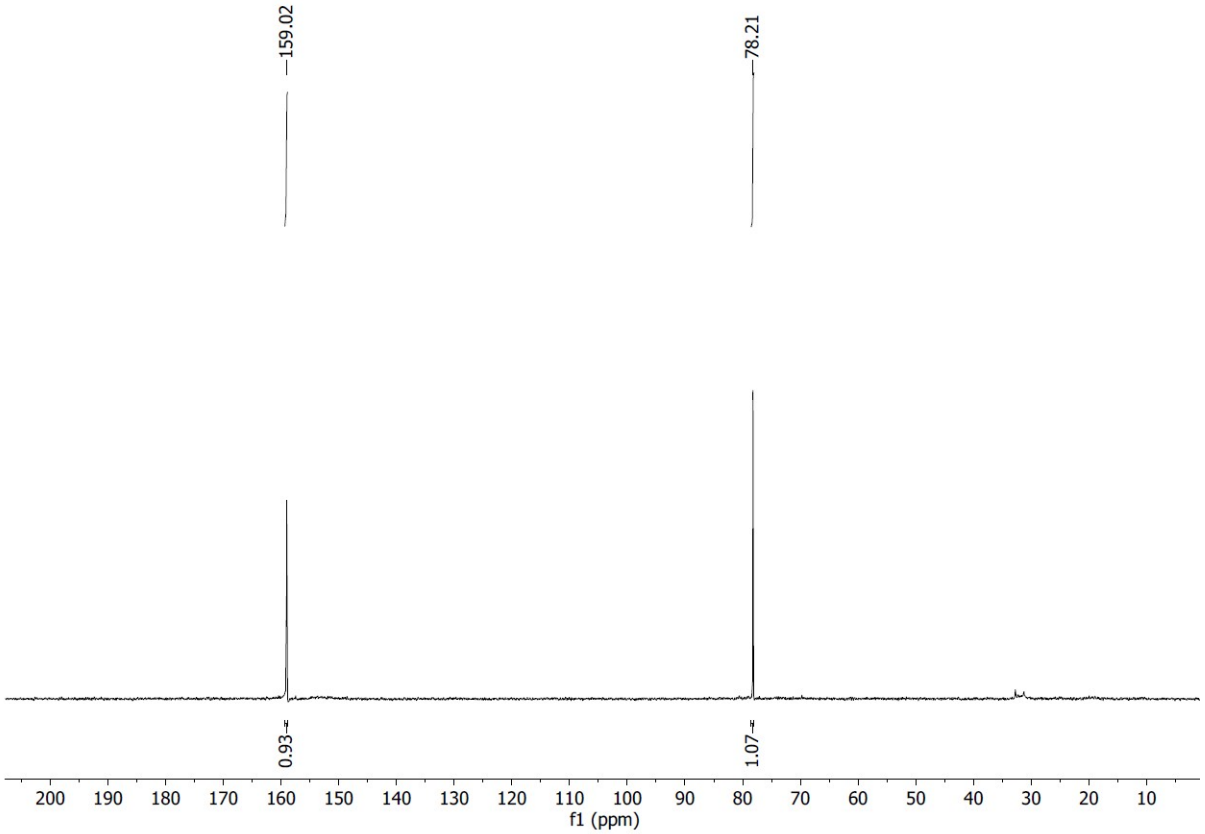

Figure S27: *$^{31}P\{^{1}H\}$ NMR (162 MHz, C_6D_6) of **3**.*

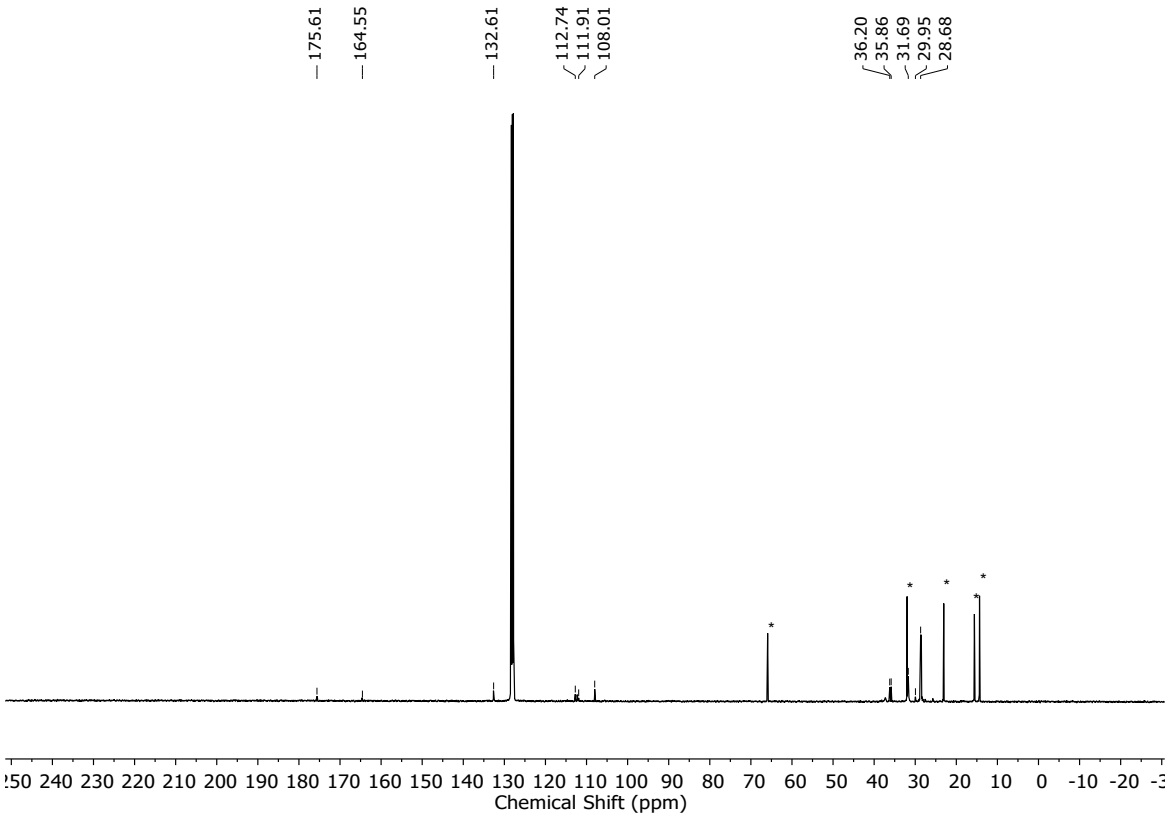

Figure S28: *$^{13}C\{^{1}H\}$ NMR (101 HZ, C_6D_6) of **3**. Resonances marked * are due to residual solvent.*

5.6 $\{(^{iPr}POCOP)TiCl_3\}_2$ (4)

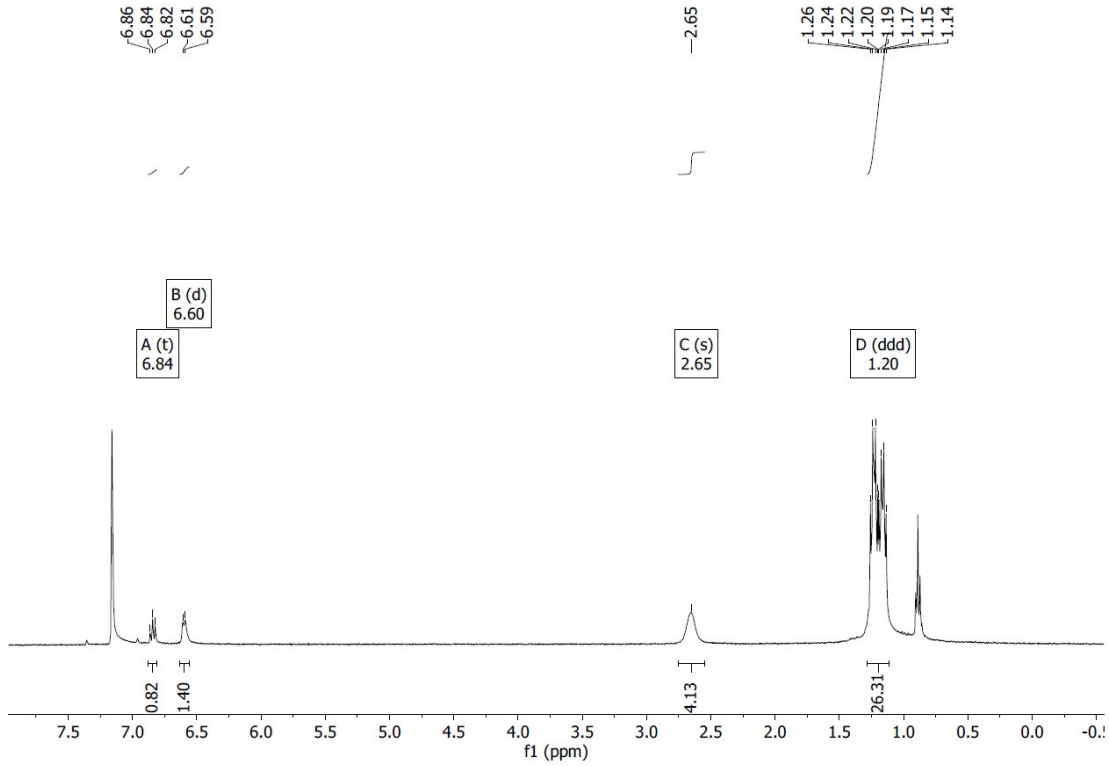

Figure S29**: ^{1}H NMR (400 MHz, C_6D_6) of **4.

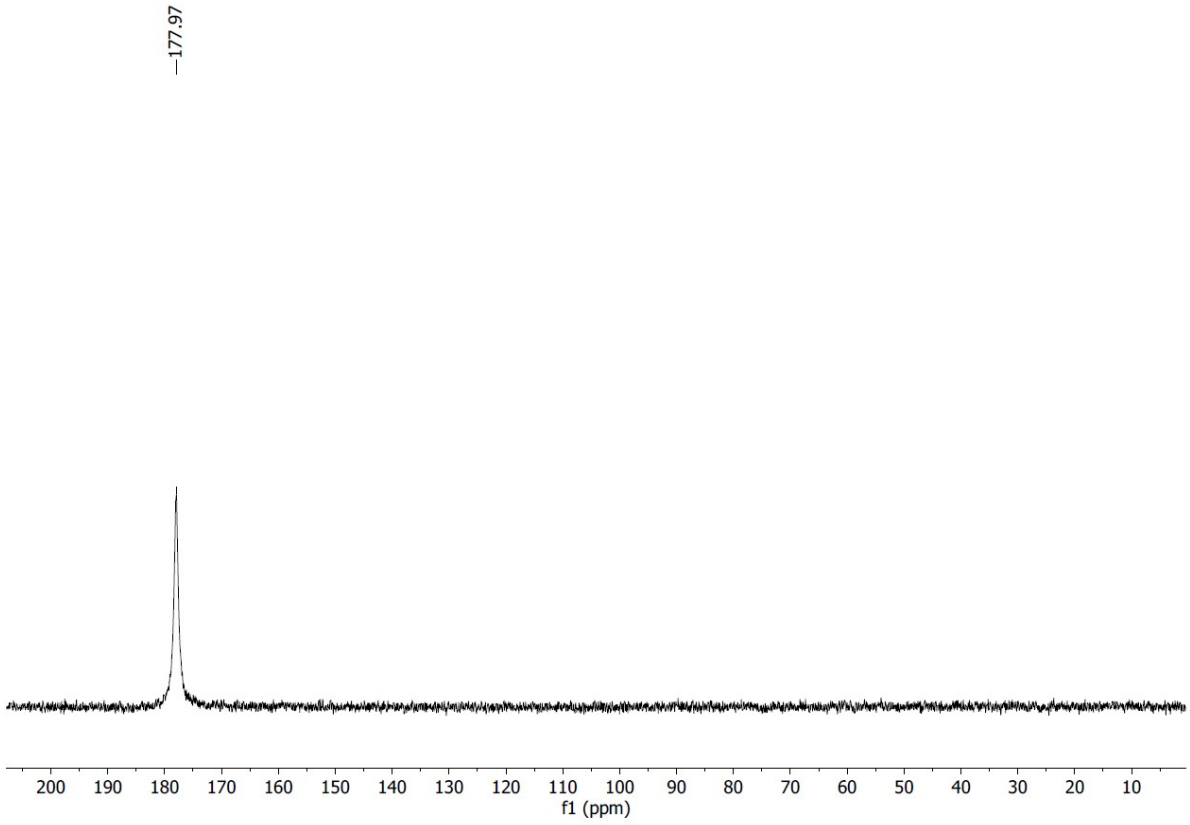

***Figure S30:** $^{31}P\{^{1}H\}$ NMR (162 MHz, C_6D_6) of **4**.*

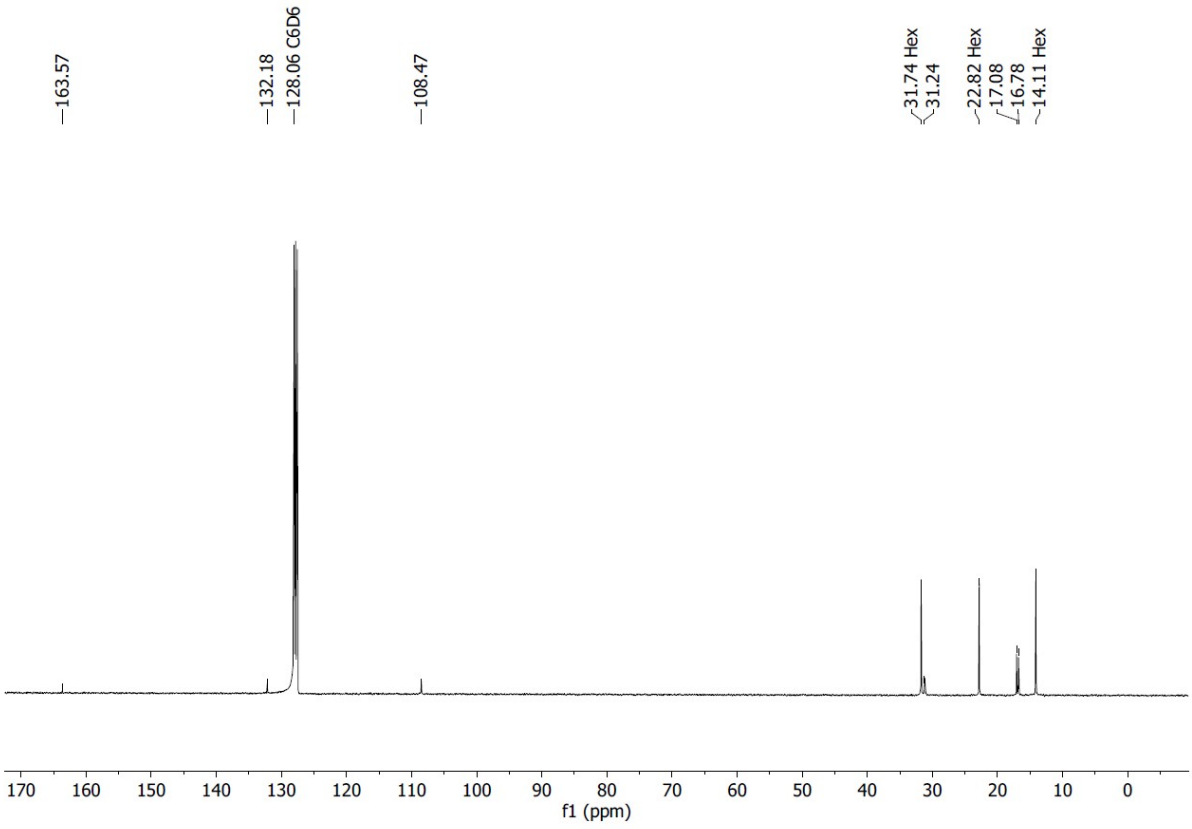

Figure S31: *^{13}C NMR (156 MHz, C_6D_6) of* ***4****.*

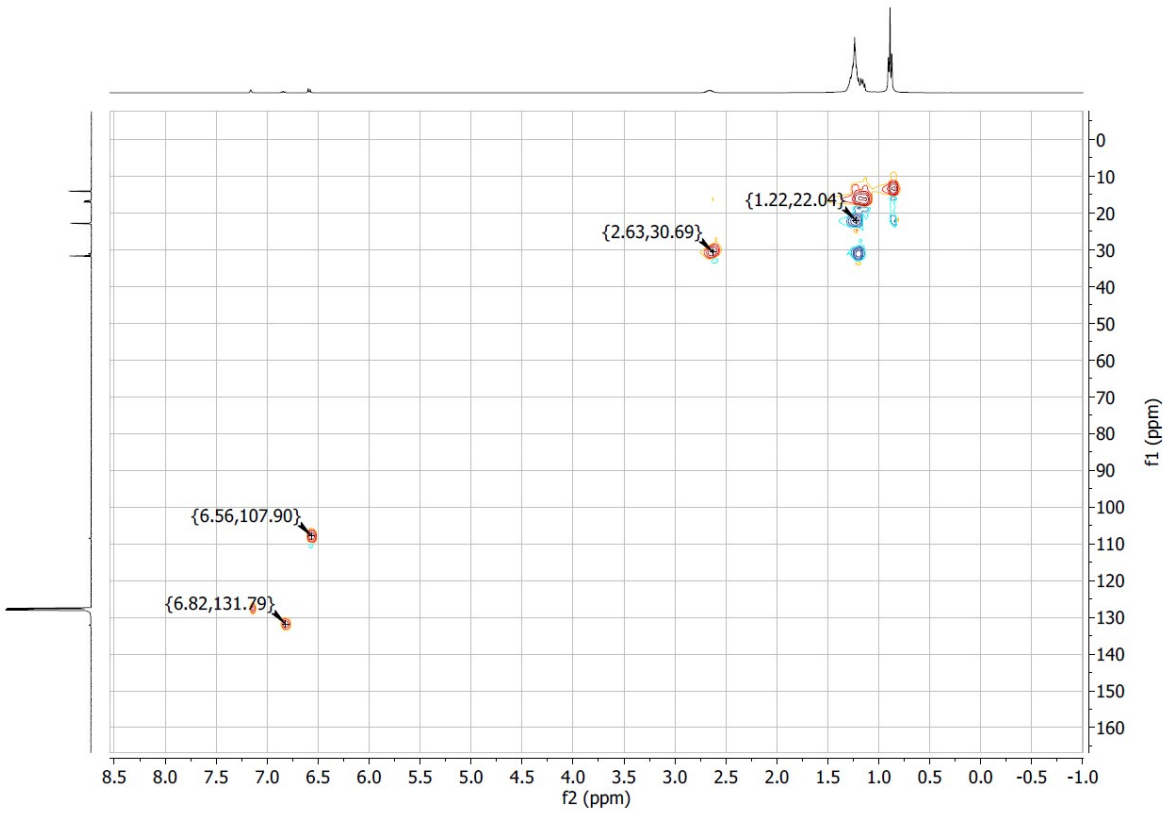

Figure S32: *HSQC NMR (C_6D_6) of* ***4.***

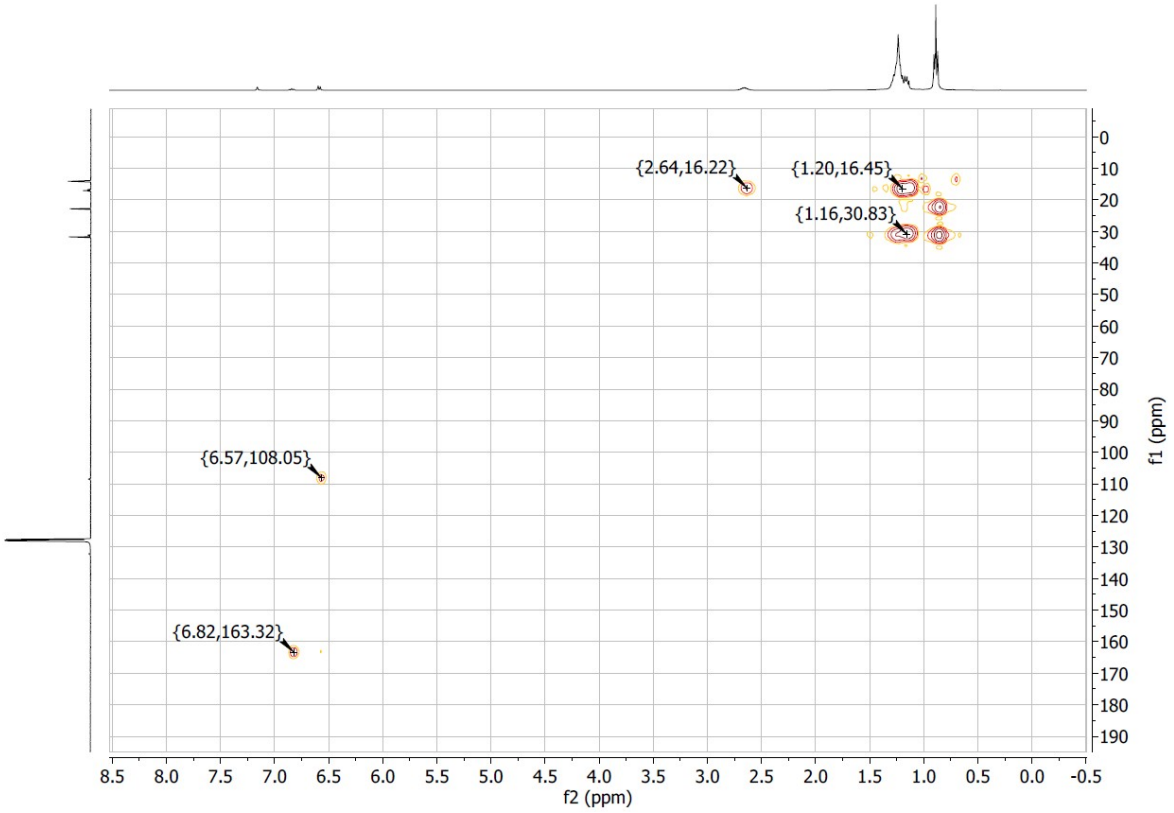

Figure S33: *HMBC NMR (C_6D_6) of* ***4****.*

5.7 (^{tBu}POCOP)TiMe$_2$ (5)

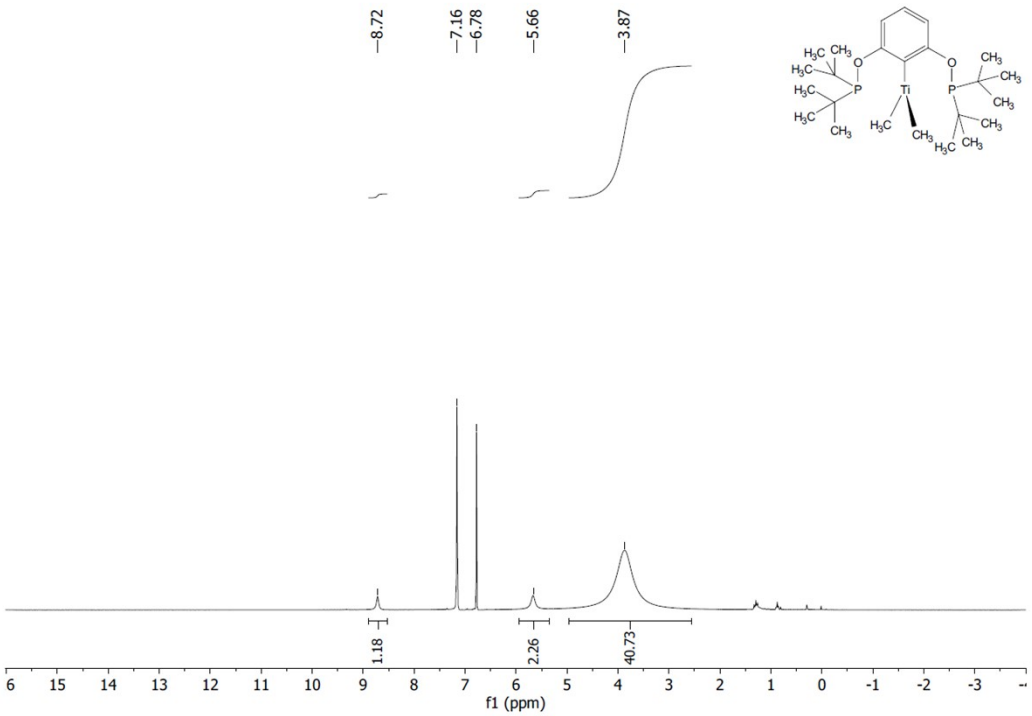

Figure S34: *Evan's ^{1}H NMR (400 MHz, C_6D_6) of* ***5****. Resonance at 6.78 ppm is due to bulk solvent, resonance at 7.16 is due to pure solvent capillary insert.*

5.8 (^{tBu}POCOP)TiPhCl (6)

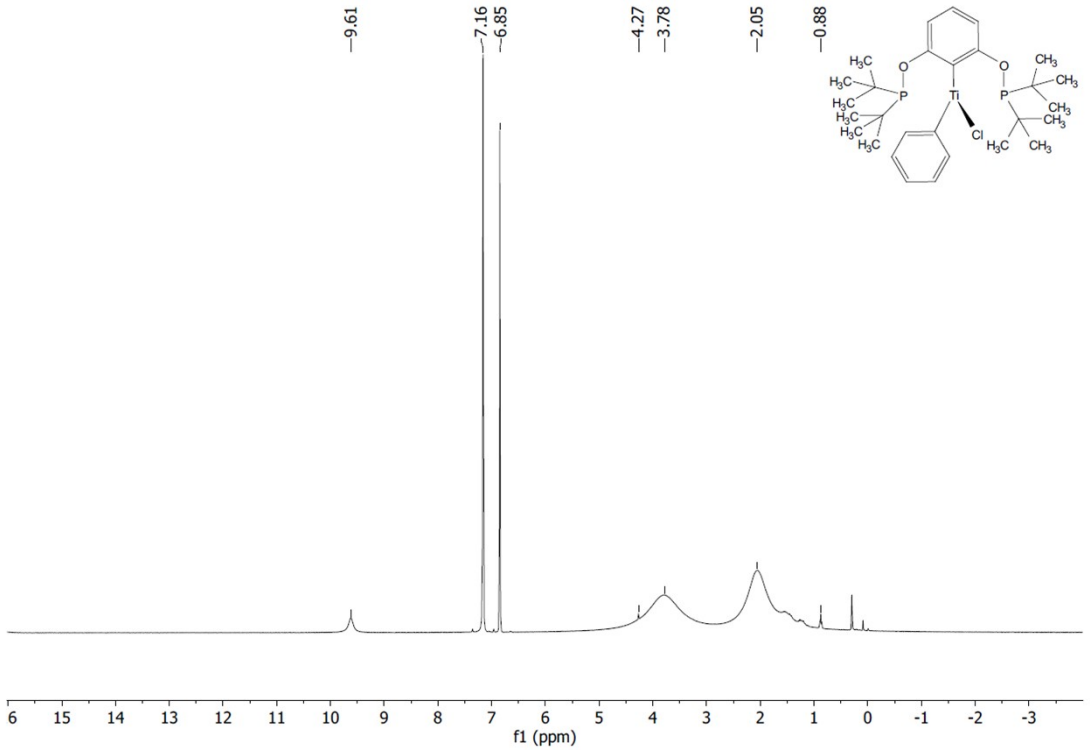

Figure S35: *Evan's ^{1}H NMR (400 MHz, C_6D_6) of **6**. Resonance at 6.85 ppm is due to bulk solvent, resonance at 7.16 is due to pure solvent capillary insert.*

5.9 (^{tBu}POCOP)TiNpCl (7)

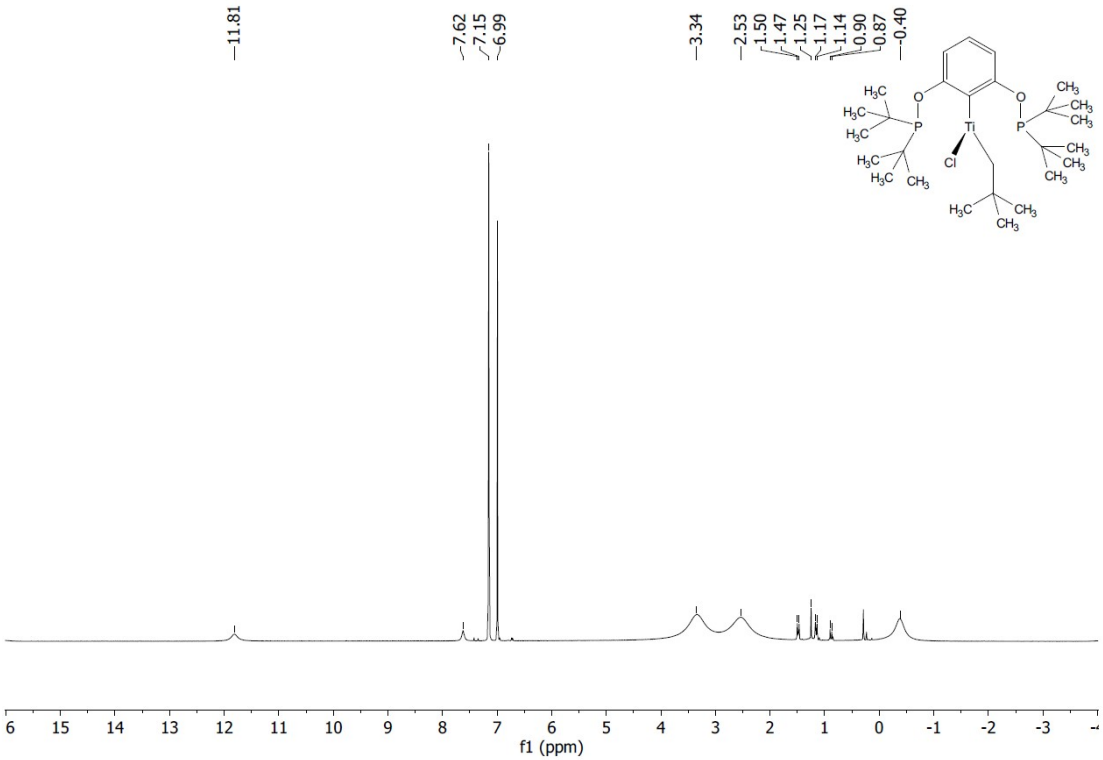

Figure S36: *^{1}H NMR (400 MHz, C_6D_6) of **7**. Resonance at 6.99 ppm is due to bulk solvent, resonance at 7.16 is due to pure solvent capillary insert*

5.10 {(^{tBu}POCOP)TiHCl}$_2$ (8)

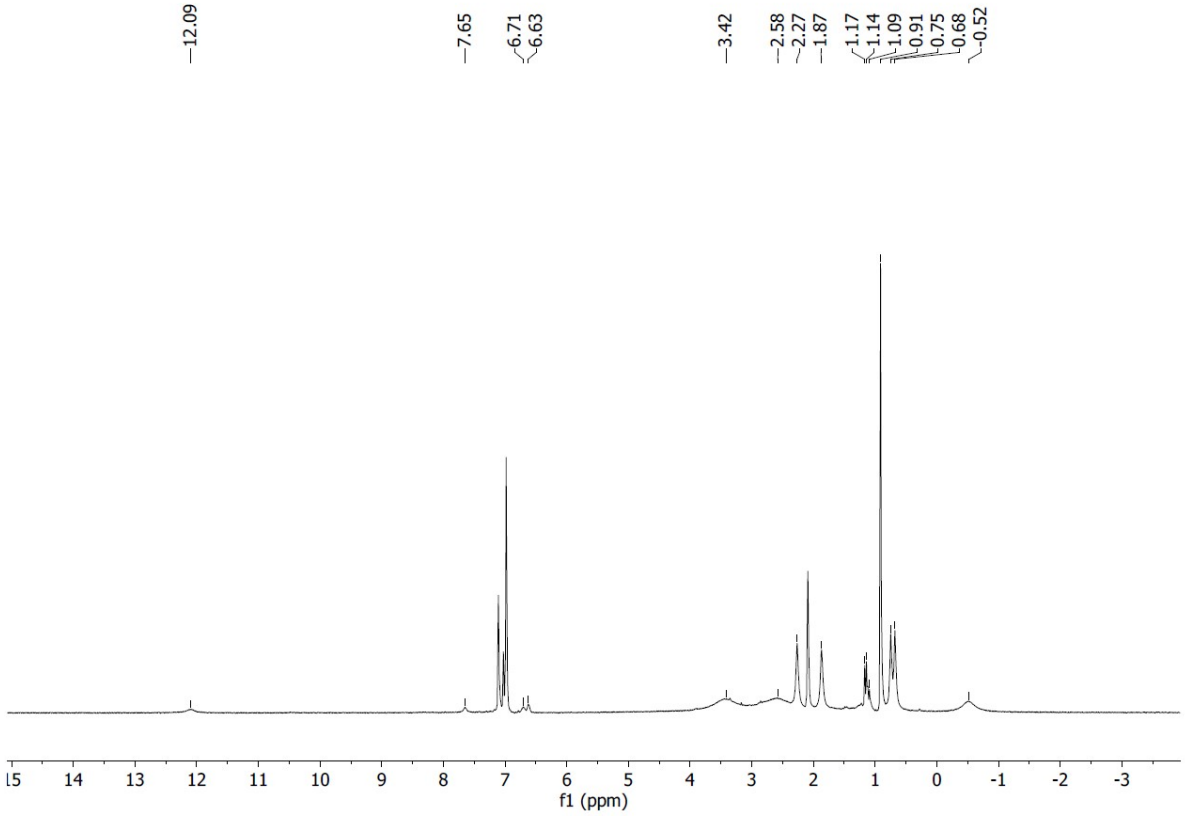

***Figure S37**: ^{1}H NMR (400 MHz, C_6D_6) of **8**. Sharp resonance at 0.91 is due to neopentane.*

6. Computational Details

6.1 Computational Methods

All electronic structure calculations were carried out using the Gaussian 16 (revision B.01) and ORCA 4.2.1 program packages.[11,12] Unconstrained optimizations of ground-state geometries and subsequent analytical frequency calculations were carried out at DFT level using the BP86 GGA exchange-correlation functional[13,14] in conjunction with Ahlrich's def2-TZVP basis set on Ti, P and Cl atoms and def2-SVP on C and H atoms.[15,16] Effects due to van-der-Waals interactions were accounted for by inclusion of Grimme's atom-pairwise dispersion correction including Becke-Johnson damping (D3BJ).[17,18] An ultrafine integration grid, corresponding to a pruned grid of 99 radial shells and 590 angular points per shell, was used for all calculations. All stationary points were confirmed to be minima or transition states by the absence of any or presence of exactly one imaginary mode in their vibrational spectra, respectively. Thermal and entropic corrections to the SCF energies (T = 298.15 K and p = 1 atm) were also extracted from the vibrational gas phase calculations. Single-point calculations for accurate energies and electronic structure analysis were performed at the B3LYP-D3/def2-TZVPP[19] level of theory utilising the previously optimised geometries. The topology of the electron density in was analysed by means of QTAIM (quantum theory of atoms in molecules),[20] as implemented in the AIMALL package.[21] Quantitative analysis of interactions between donor and acceptor orbitals within the framework of second order perturbation theory was performed with NBO 6.0.[22] Electron Paramagnetic Resonance (EPR) parameters (g-tensor, hyperfine coupling constants) were calculated with the ORCA package using the PBE0 functional[23] combined with the def-TZVP basis set for Ti and P and the def2-SVP basis set for the remaining atoms. The RIJCOSX approximation was employed and supplemented with the def2/J auxiliary basis sets.

6.2 Optimised Geometries

Table S1: Comparison of selected calculated and experimental bond parameters of complexes **1**–**4** (BP86-D3/def2-TZVP/def2-SVP).

	Exp.	**DFT**
1		
Ti(1)–P(1)	2.5825(7)	2.542
Ti(1)–P(2)	2.6026(7)	2.542
Ti(1)–Cl(1)	2.2917(7)	2.314
Ti(1)–Cl(2)	2.3177(7)	2.264
Ti(1)–C(1)	2.1960(2)	2.210
P(1)–Ti(1)–P(2)	142.16(3)	142.26
2		
Ti(1)–P(1)	2.6133(11)	2.580
Ti(1)–P(2)	2.6330(11)	2.612
Ti(1)–Cl(1)	2.2643(11)	2.267
Ti(1)–Cl(2)	2.3831(10)	2.356
Ti(1)–Cl(3)	2.3006(10)	2.309
Ti(1)–C(1)	2.2081(11)	2.220
C(1)–Ti(1)–P(1)	71.80(4)	72.39
C(1)–Ti(1)–P(2)	68.64(4)	69.38
P(1)–Ti(1)–Cl(2)	79.55(3)	78.43
P(2)–Ti(1)–Cl(2)	144.47(4)	143.88
Cl(1)–Ti(1)–Cl(3)	143.16(4)	144.36
3		
Ti(1)–P(1)	2.746(5)	2.715
Ti(1)–P(3)	2.754(5)	2.715
Ti(1)–Cl(1)	2.306(6)	2.319
Ti(1)–Cl(2)	2.315(6)	2.319
Ti(1)–O(1)	1.822(14)	1.876
Ti(1)–O(3)	1.831(13)	1.876
P(1)–Ti(1)–P(3)	178.4(2)	171.79
P(1)–Ti(1)–O(1)	71.3(4)	71.31
Cl(1)–Ti(1)–Cl(2)	95.3(2)	100.32
O(1)–Ti(1)–O(3)	89.5(6)	88.07
4		
Ti(1)–Cl(1)	2.293(1)	2.276
Ti(1)–Cl(2)	2.336(1)	2.301
Ti(1)–Cl(3)	2.587(1)	2.543
Ti(1)–P(1)	2.578(1)	2.558
Ti(1)–P(2)	2.587(1)	2.568
Ti(1)–C(1)	2.252(4)	2.280
Ti(1)-Ti(1')	4.116(1)	4.010
Cl(1)-Ti(1)-Cl(2)	174.05(5)	175.11

Table S2: Comparison of selected calculated and experimental bond parameters of complexes **5**–**7** (BP86-D3/def2-TZVP/def2-SVP).

	Exp.	**DFT**
5		
Ti(1)–P(1)	2.6243(9)	2.559
Ti(1)–P(2)	2.6180(9)	2.559
Ti(1)–C(1)	2.138(4)	2.115
Ti(1)–C(2)	2.143(4)	2.154
Ti(1)–C(3)	2.241(3)	2.252
P(1)–Ti(1)–P(2)	141.44(3)	140.52
C(2)-Ti(1)-C(3)	140.53(14)	141.38
6		
Ti(1)–P(1)	2.6109(6)	2.551
Ti(1)–P(2)	2.6141(6)	2.551
Ti(1)–C(1)	2.2129(19)	2.216
Ti(1)–C(23)	2.100(2)	2.069
Ti(1)–Cl(1)	2.3156(6)	2.302
P(1)–Ti(1)–P(2)	143.72(2)	144.03
C(1)–Ti(1)–Cl(1)	144.36(5)	146.12
7		
Ti(1)–P(1)	2.6223(17)	2.564
Ti(1)–P(2)	2.6232(17)	2.559
Ti(1)–C(1)	2.033(6)	2.041
Ti(1)–C(6)	2.222(5)	2.225
Ti(1)–Cl(1)	2.3799(14)	2.341
P(1)–Ti(1)–P(2)	139.03(6)	139.75
C(6)–Ti(1)–Cl(1)	140.40(15)	139.77
Ti(1)–C(1)–C(2)	156.3(5)	149.17
8		
Ti(1)–Ti(2)	3.1708(12)	2.918
Ti(1)–P(1)	2.6858(13)	2.647
Ti(1)–P(2)	2.6898(13)	2.622
Ti(1)–C(1)	2.212(4)	2.208
Ti(2)–P(3)	2.6906(13)	2.647
Ti(2)–P(4)	2.6799(13)	2.621
Ti(2)–C(23)	2.221(4)	2.208
Ti(1)–Cl(1)	2.3157(14)	2.316
Ti(2)–Cl(2)	2.3113(14)	2.316
P(1)–Ti(1)–P(2)	138.03(5)	138.44
C(1)–Ti(1)–Cl(1)	129.99(14)	128.29
P(3)–Ti(2)–P(4)	137.77(5)	138.43
C(23)–Ti(1)–Cl(2)	129.79(13)	128.27

Table S3: Comparison of selected bond distance in dependence of DFT functional for complex **8** (functional/def2-SVP).

Functional	Ti–Ti	Ti(1)–H(1)	Ti(1)–H(2)	Ti(2)–H(1)	Ti(2)–H(2)
B3LYP (20%)	3.177	1.843	1.894	1.885	1.897
B3LYP–D3(BJ)	3.100	1.822	1.865	1.850	1.863
BP86 (0%)	2.977	1.839	1.859	1.859	1.839
BP86–D3(BJ)	2.892	1.819	1.839	1.840	1.819
B97–D3 (0%)	2.917	1.811	1.838	1.838	1.811
M06 (27%)	3.044	1.851	1.880	1.844	1.852
M06–D3	3.038	1.850	1.877	1.841	1.849
M06L (0%)	2.936	1.839	1.864	1.864	1.839
M06L–D3	2.933	1.838	1.863	1.863	1.838
M062X (54%)	3.141	1.847	1.885	1.884	1.898
M062X–D3	3.138	1.846	1.884	1.882	1.897
MN15 (44%)	3.111	1.824	1.875	1.851	1.862
TPSS (0%)	2.962	1.840	1.861	1.861	1.840
TPSS–D3(BJ)	2.903	1.826	1.848	1.848	1.826
TPSSh (10%)	3.140	1.846	1.890	1.873	1.885
ωB97xD (22%)	2.891	1.788	1.863	1.864	1.788

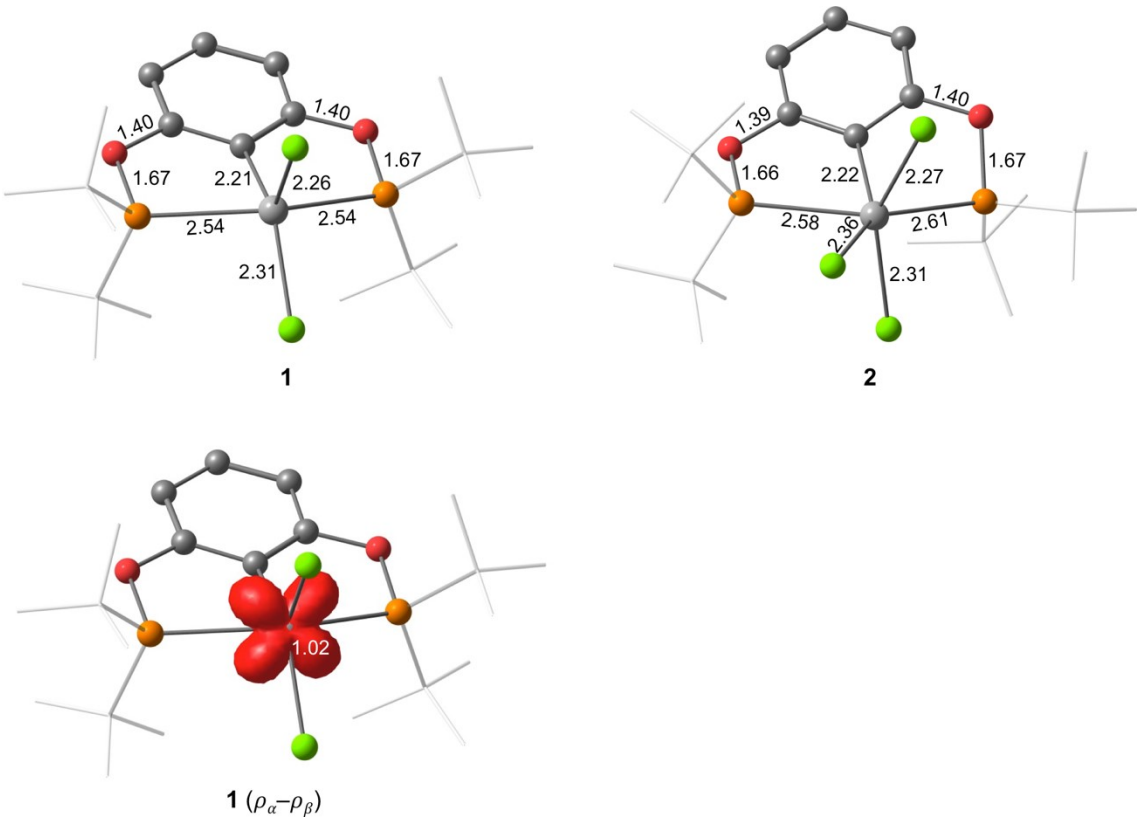

Figure S38: *Optimised geometries (BP86-D3/def2-TZVP/def2-SVP) of complexes **1** and **2** (bond distances in Å). along with spin density plot for complex **1** (isovalue 0.01 au).*

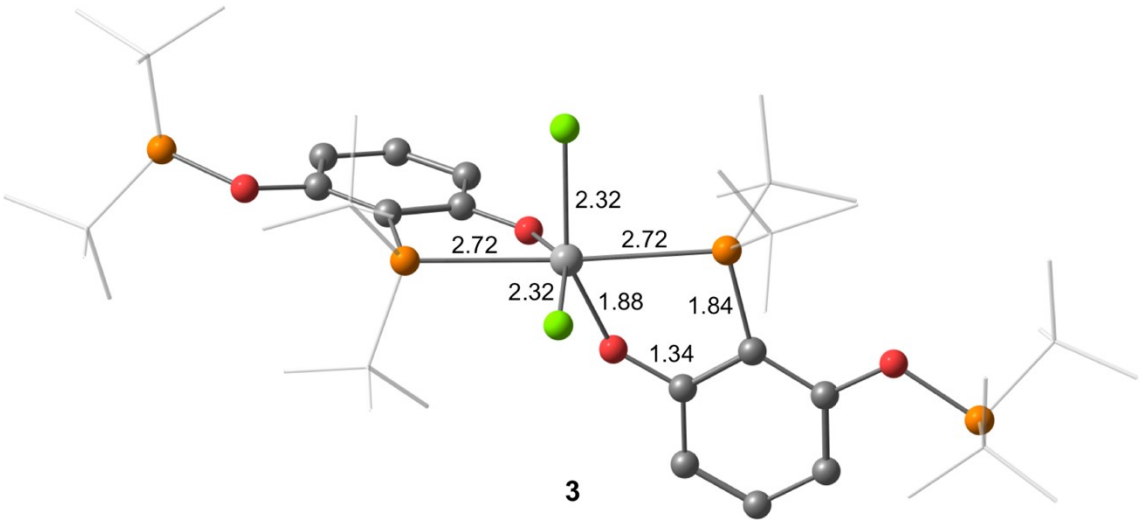

Figure S39: *Optimised geometry (BP86-D3/def2-TZVP/def2-SVP) of complex **3** (bond distances in Å).*

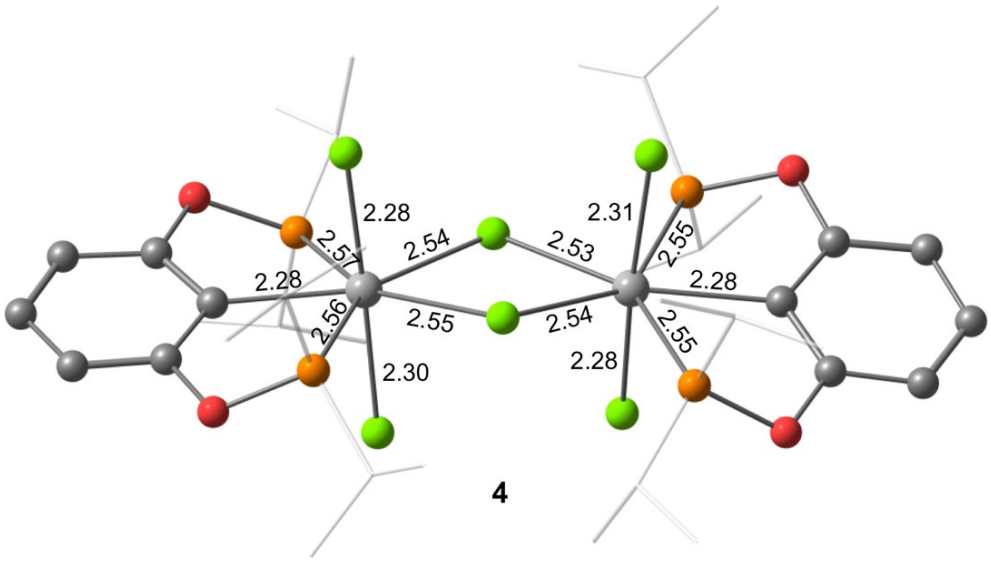

Figure S40: *Optimised geometry (BP86-D3/def2-TZVP/def2-SVP) of complex **4** (bond distances in Å).*

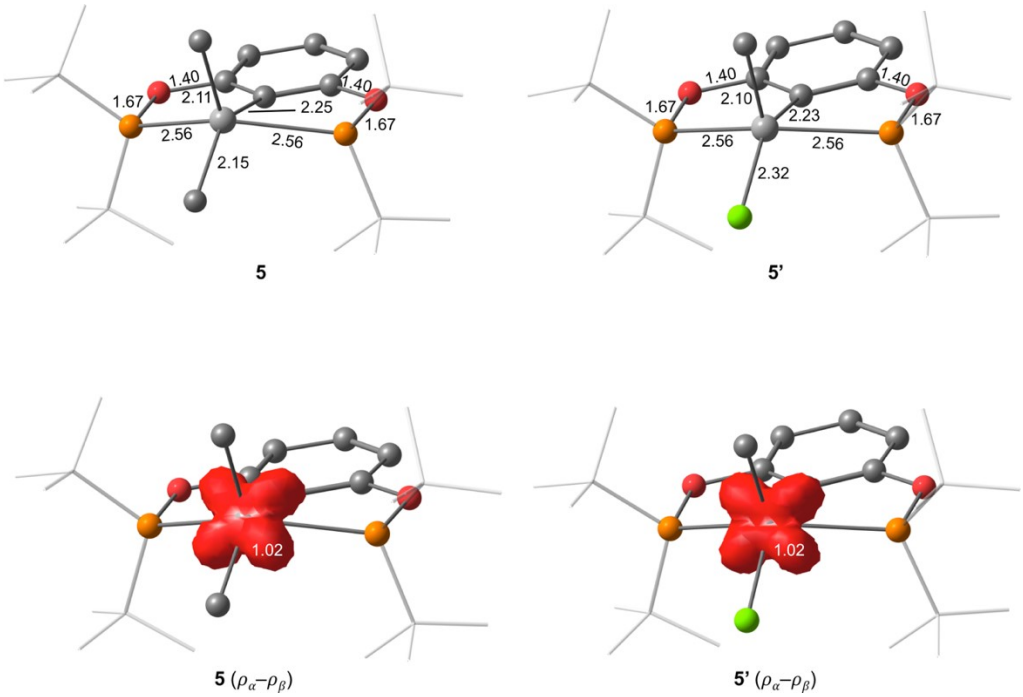

Figure S41: *Optimised geometries (BP86-D3/def2-TZVP/def2-SVP) of complexes* ***5*** *and* ***5'*** *(bond distances in Å) along with spin density plots (isovalue 0.01 au).*

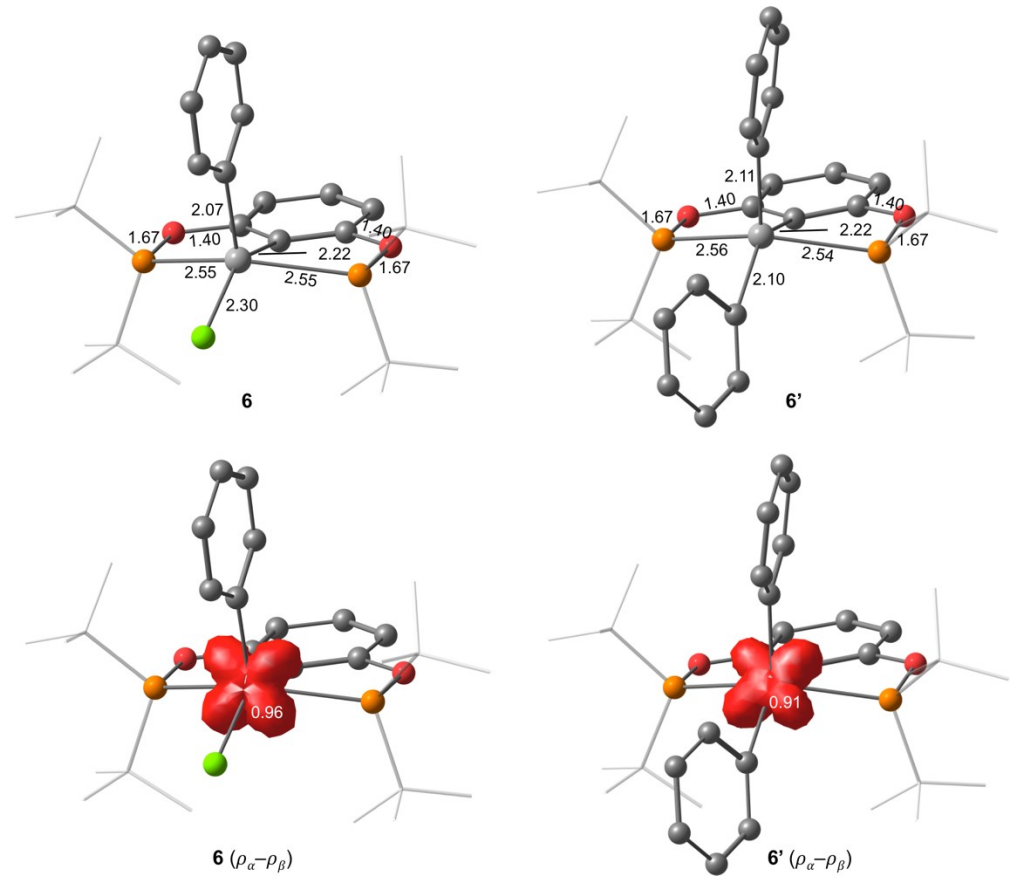

Figure S42: *Optimised geometries (BP86-D3/def2-TZVP/def2-SVP) of complexes* ***6*** *and* ***6'*** *(bond distances in Å) along with spin density plots (isovalue 0.01 au).*

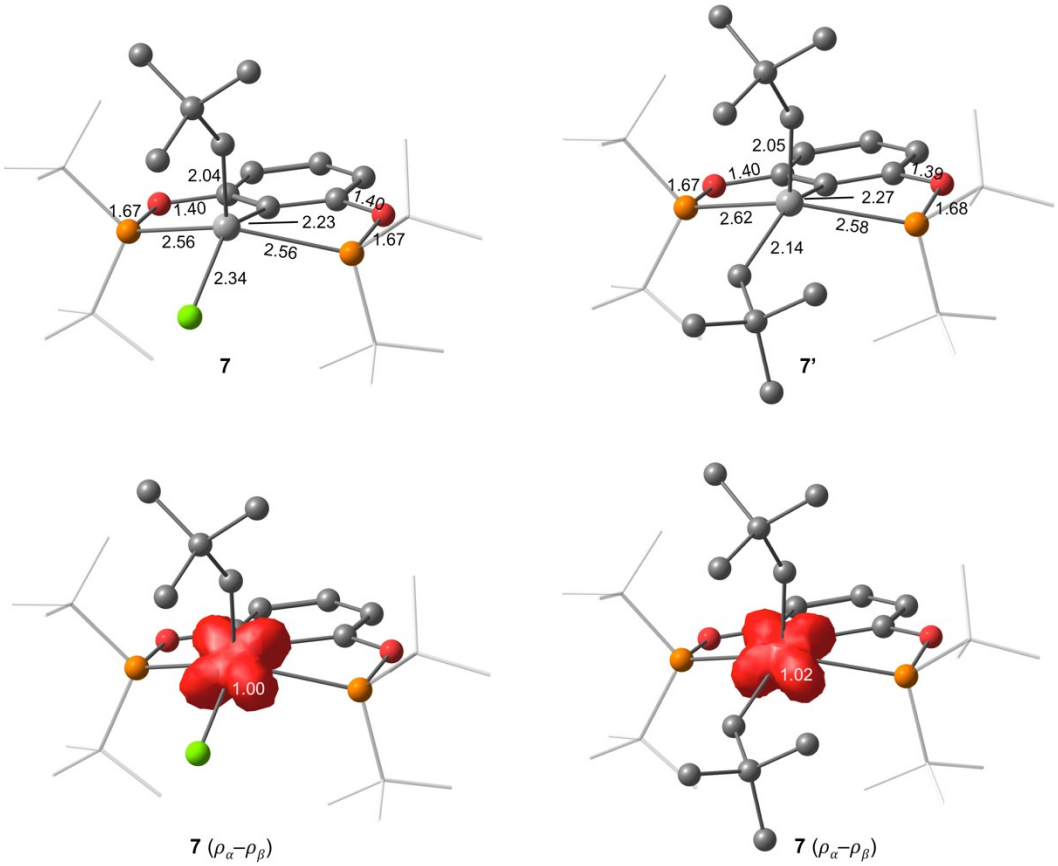

Figure S43: Optimised geometries (BP86-D3/def2-TZVP/def2-SVP) of complexes **7** and **7'** (bond distances in Å) along with spin density plots (isovalue 0.01 au).

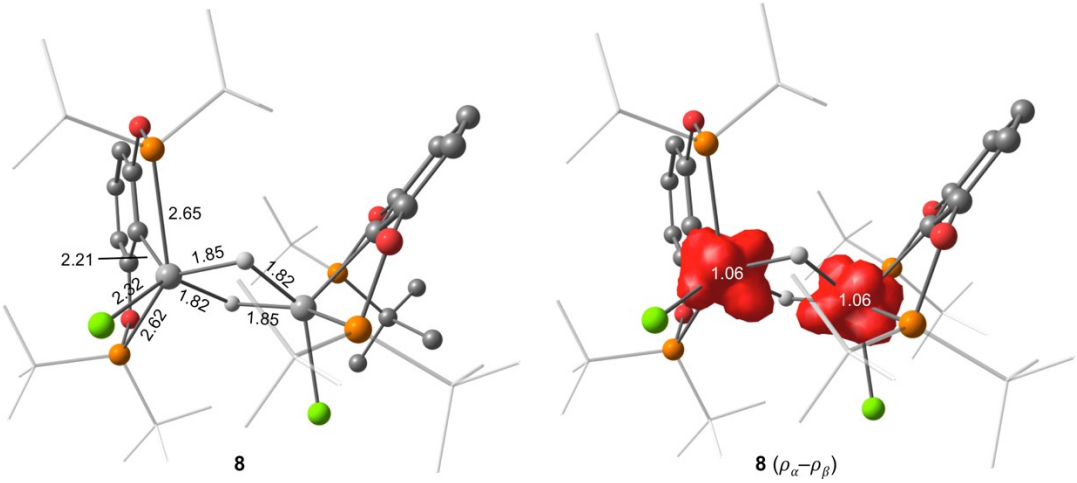

Figure S44: *Optimised geometries (BP86-D3/def2-TZVP/def2-SVP) of complex* ***8*** *(bond distances in Å) along with spin density plot (isovalue 0.01 au).*

6.3 Calculated EPR Parameters

Table S4: Comparison of calculated and experimental isotropic *g*-values and hyperfine coupling constants (in MHz and mT).

Complex	**g_{iso} / ppm**		**a_0 / mT (MHz)**	
	exp.	**calc.**	**exp.**	**calc.**
1	1.9665	1.9698	2.31 (63.6)	2.76 (76.2)
5	1.9700	1.9749	2.25 (62.1) 0.64 (17.7)	2.80 (77.3) 0.38 (10.4)
6	1.9665 1.9720	1.9724	2.26 (62.2) 2.24 (61.8)	2.72 (75.2)
7	1.9665	1.9778	2.20 (60.6)	2.68 (74.3)

6.4 Analysis of the electronic structure of 7

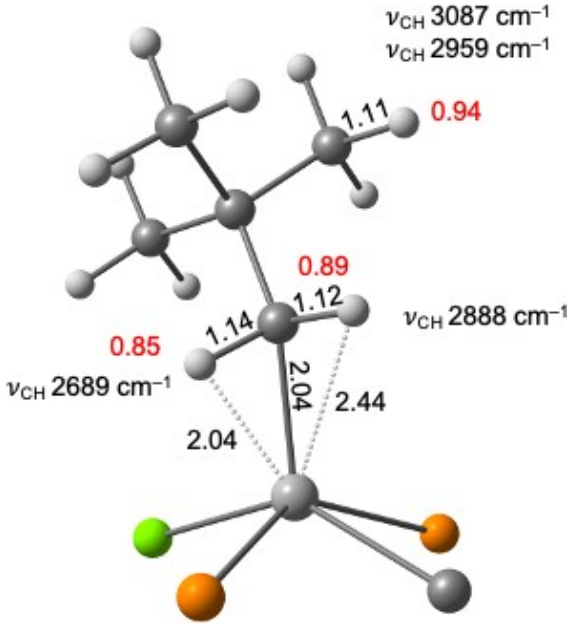

Figure S45: *Optimised geometry (BP86-D3/def2-TZVP/def2-SVP) of the {Ti(Cl)P$_2$(Np)C$_{Ph}$} unit in complex **7**. Key bond distances (Å) are given along with vibrational frequencies and Wiberg Bond Orders for C–H bonds.*

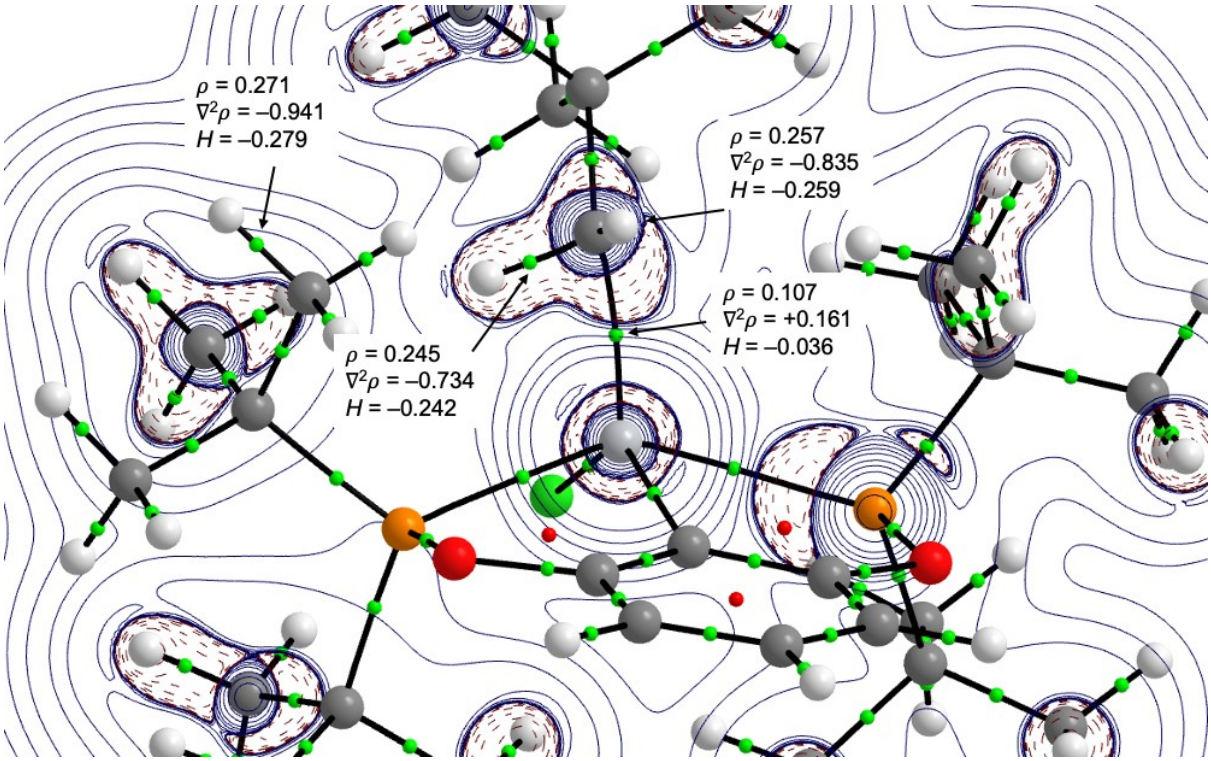

Figure S46: *Contour map of the Laplacian of the electron density, $\nabla^2\rho(\mathbf{r})$ in the Ti–C(1)–H(1) plane of **7**, with projected stationary points and bond paths (B3LYP-D3/def2-TZVPP). Bond critical points (BCP) are shown in green whilst ring critical points (RCP) are shown in red. Calculated QTAIM parameters (a.u.) for selected BCPs are shown as $\sigma(\mathbf{r})$ = electron density, $\nabla^2\rho(\mathbf{r})$ = Laplacian of electron density and $H(\mathbf{r})$ = local energy density.*

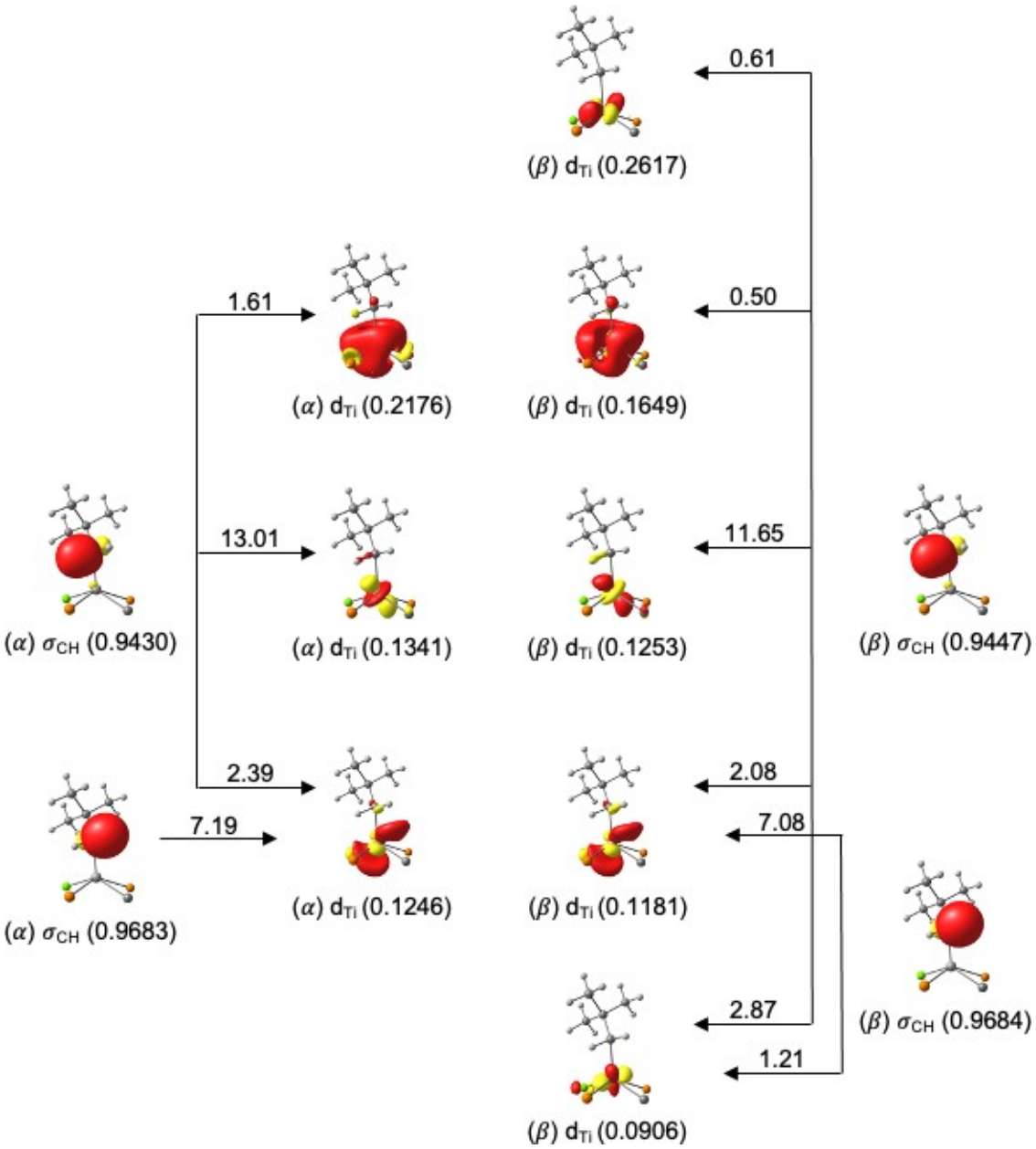

Figure S47: *Leading NBO donor-acceptor orbitals (B3LYP-D3/def2-TZVPP) between the neopentyl unit and the Ti centre in* ***7*** *(isovalue 0.05 a.u.). Interaction energies from second-order perturbation theory (kcal mol^{-1}) and natural occupations numbers are also included.*

6.5 Effect of Different Phosphine Substituents on Dimerization

The effect of the phosphine substituent groups on the thermodynamic dimerization equilibrium shown in Scheme S1 was probed by varying R (H, CH_3, ^{i}Pr). In these ligand systems the dimer is the favourable and lower energy conformer, with Gibb's free energies of −19 kcal mol^{-1}, −19 kcal mol^{-1} and −15 kcal mol^{-1} respectively. In contrast, with R = ^{t}Bu groups, the monomer is the preferred and lower energy conformer, with a Gibb's free energy change of dimerization of +1 kcal mol^{-1}. This is also shown in a greater titanium-titanium distance of 4.12 Å versus 4.01 Å (CH_3 and ^{i}Pr) or 3.93 Å (H) shown in Table 1.

Scheme S1: Dimerization of $TiCl_3$(POCOP) complexes.

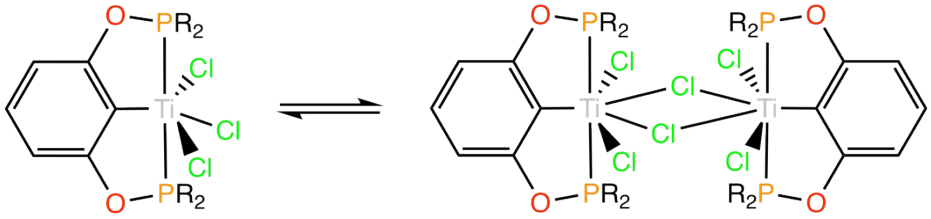

Table S5: Computed enthalpies **Δ***H* and free energy values **Δ***G* of dimerization for selected POCOP ligand systems carrying different substituents R. For each dimer, Ti–Ti distances are given along with Ti–Cl_{bridge} distances averaged over four $Ti_2(\mu_2\text{-}Cl)_2$ bonds.

R	**Δ***H* (**Δ***G*) / kcal mol^{-1}	**Ti–Ti / Å**	**Ti–Cl / Å**
H	–28.3 (–15.7)	3.93	2.57
CH_3	–26.5 (–13.7)	4.01	2.56
^{i}Pr	–22.2 (–6.2)	4.01	2.54
^{t}Bu	–10.1 (+8.3)	4.12	2.58

6.6 Mechanism of hydrogen activation by 7

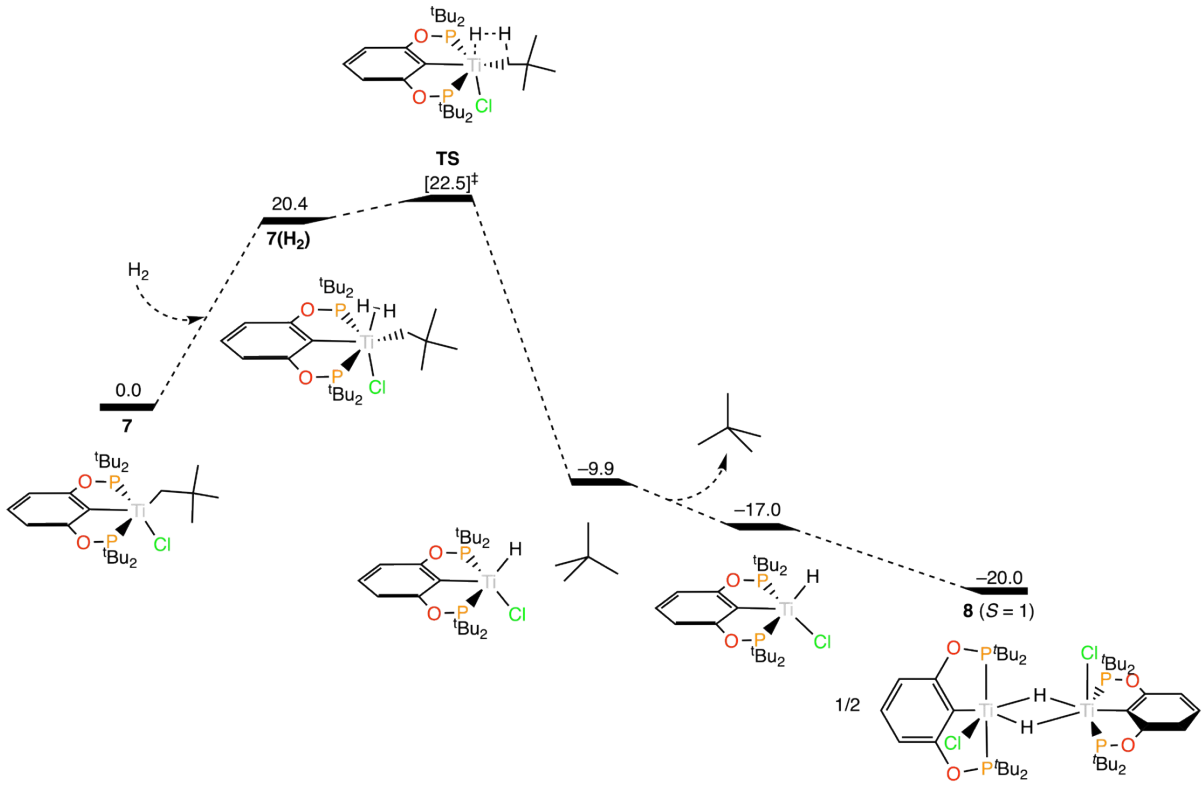

Figure S48: *Calculated Gibbs Free Energy diagram (B3LYP-D3(BJ)/def2-TZVPP) for hydrogen activation by* ***7*** *yielding dimeric* ***8****. Energies in kcal mol^{-1}.*

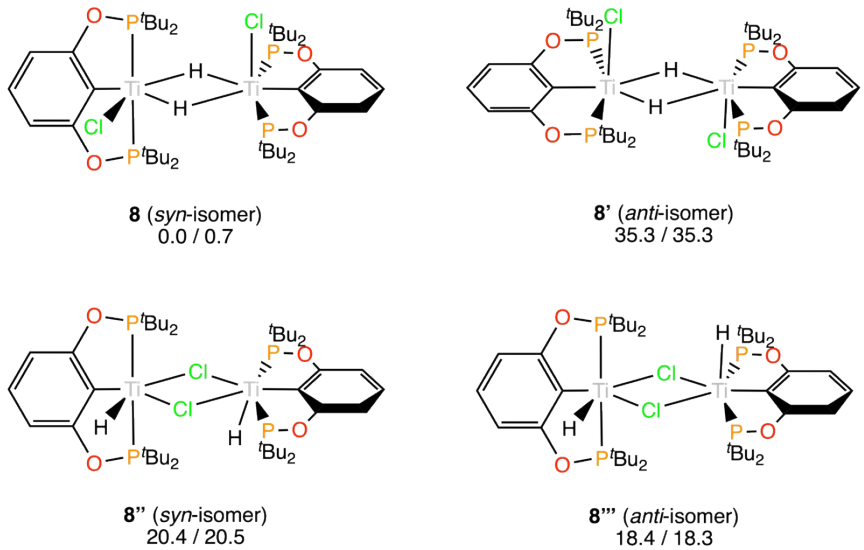

Figure S49: *Calculated relative Gibbs Free Energies (B3LYP-D3/def2-TZVP/def2-SVP) for isomers of complex* ***8*** *in their broken-symmetry singlet (M_s = 0) / triplet state (S = 1). Singlepoint energies were computed with ORCA 4.2.1 on the triplet geometries optimised with Gaussian.*

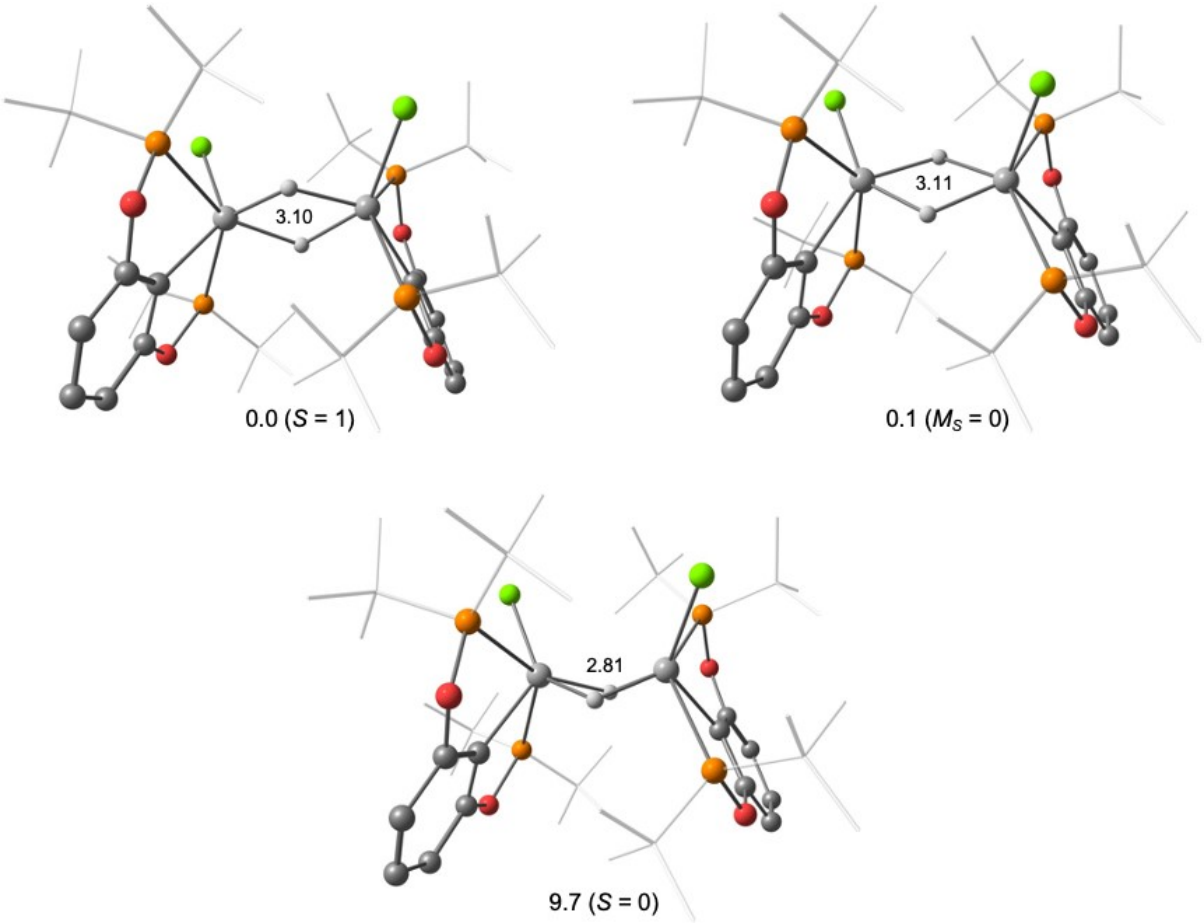

Figure S50: *Optimised geometries (ORCA 4.2.1, B3LYP-D3/def2-TZVP/def2-SVP) of complex 8 in triplet (S = 1), broken-symmetry singlet (M_s = 0) and closed-shell singlet (S = 0) states. Relative energies in kcal mol^{-1} are given along with Ti-Ti distances.*

7. References

1 E. M. Schubert, *J. Chem. Educ.*, 1992, **69**, 62.
2 Oxford Diffraction Ltd., 2011.
3 L. Palatinus and G. Chapuis, *J. Appl. Crystallogr.*, 2007, **40**, 786–790.
4 R. I. Cooper, A. L. Thompson and D. J. Watkin, *J. Appl. Crystallogr.*, 2010, **43**, 7.
5 P. W. Betteridge, J. R. Carruthers, R. I. Cooper, K. Prout and D. J. Watkin, *J. Appl. Crystallogr.*, 2003, **36**, 1487–1487.
6 S. Stoll and A. Schweiger, *J. Magn. Reson.*, 2006, **178**, 42–55.
7 L. E. Manzer, *Inorg. Synth.*, 1982, **21**, 135–140.
8 D. Himmelbauer, B. Stöger, L. F. Veiros, M. Pignitter and K. Kirchner, *Organometallics*, 2019, **38**, 4669–4678.
9 R. R. Schrock and J. D. Fellmann, *J. Am. Chem. Soc.*, 1978, **100**, 3359–3370.
10 T. R. Hoye, B. M. Eklov and M. Voloshin, *Org. Lett.*, 2004, **6**, 2567–2570.
11 J. Zhang, W. Huang, K. Han, G. Song and S. Hu, *Dalt. Trans.*, 2022, **51**, 12250–12257.
12 F. Neese, F. Wennmohs, U. Becker, C. Riplinger, *J. Chem. Phys.*, 2020, **152**, 224108.
13 A. D. Becke, *Phys. Rev. A*, 1988, **38**, 3098–3100.
14 J. P. Perdew, *Phys. Rev. B*, 1986, **33**, 8822–8824.
15 F. Weigend, R. Ahlrichs, *Phys. Chem. Chem. Phys.*, 2005, **7**, 3297–3305.
16 K. Eichkorn, F. Weigend, O. Treutler, R. Ahlrichs, *Theor. Chem. Acc.*, 1997, **97**, 119–124.
17 S. Grimme, J. Antony, S. Ehrlich, H. Krieg, *J. Chem. Phys.*, 2010, **132**, 154104.
18 S. Grimme, S. Ehrlich, L. Goerigk, *J. Comput. Chem.*, 2011, **32**, 1456–1465.
19 P. J. Stephens, F. J. Devlin, C. F. Chabalowski and M. J. Frisch, *J. Phys. Chem.*, 1994, **98**, 11623−11627.
20 R. Bader, *Chem. Rev.*, 1991, **91**, 893–928.
21 AIMAll (Version 19.10.12), Todd A. Keith, TK Gristmill Software, Overland Park KS, USA, **2019** (aim.tkgristmill.com)
22 NBO 6.0, E. D. Glendening, J. K. Badenhoop, A. E. Reed, J. E. Carpenter, J. A. Bohmann, C. M. Morales, C. R. Landis, F. Weinhold (Theoretical Chemistry Institute, University of Wisconsin, Madison, WI, **2013**); http://nbo6.chem.wisc.edu
23 C. Adamo and V. Barone, *J. Chem. Phys.*, 1999, **110**, 6158–6169.